LEVEL II

12

ARL-TR-81-37

Copy No. 76

MEASUREMENTS AND ANALYSIS OF ACOUSTIC BOTTOM INTERACTION IN THE NORTHWESTERN MEXICAN BASIN

Michael W. Hooper
Gregory D. Ingram
Stephen K. Mitchell

APPLIED RESEARCH LABORATORIES
THE UNIVERSITY OF TEXAS AT AUSTIN
POST OFFICE BOX 8029, AUSTIN, TEXAS 78712

5 October 1981

Technical Report

APPROVED FOR PUBLIC RELEASE;
DISTRIBUTION UNLIMITED.

Prepared for:

NAVAL OCEAN RESEARCH
AND DEVELOPMENT ACTIVITY
NSTL STATION, MS 39529

18

UNCLASSIFIED

SECURITY CLASSIFICATION OF THIS PAGE (When Data Entered)

REPORT DOCUMENTATION PAGE	READ INSTRUCTIONS BEFORE COMPLETING FORM
1. REPORT NUMBER	2. GOVT ACCESSION NO. AD-A107 551 / 3. RECIPIENT'S CATALOG NUMBER
4. TITLE (and Subtitle) MEASUREMENTS AND ANALYSIS OF ACOUSTIC BOTTOM INTERACTION IN THE NORTHWESTERN MEXICAN BASIN	5 TYPE OF REPORT & PERIOD COVERED technical report
	6. PERFORMING ORG. REPORT NUMBER ARL-TR-81-37 /
7. AUTHOR(s) Michael W. Hooper, Gregory D. Ingram, Stephen K. Mitchell	8. CONTRACT OR GRANT NUMBER(s) N00014-78-C-0329
9. PERFORMING ORGANIZATION NAME AND ADDRESS Applied Research Laboratories, The University of Texas at Austin, Austin, TX 78712	10 PROGRAM ELEMENT, PROJECT, TASK AREA & WORK UNIT NUMBERS
11. CONTROLLING OFFICE NAME AND ADDRESS Naval Ocean Research and Development Activity, NSTL Station, MS 39529	12. REPORT DATE 5 October 1981
	13. NUMBER OF PAGES 49
14 MONITORING AGENCY NAME & ADDRESS(if different from Controlling Office)	15 SECURITY CLASS. (of this report) UNCLASSIFIED
	15a. DECLASSIFICATION DOWNGRADING SCHEDULE

16. DISTRIBUTION STATEMENT (of this Report)

Approved for public release; distribution unlimited.

17. DISTRIBUTION STATEMENT (of the abstract entered in Block 20, if different from Report)

18. SUPPLEMENTARY NOTES

19 KEY WORDS (Continue on reverse side if necessary and identify by block number)

bottom loss
Gulf of Mexico
geoacoustic model

20 ABSTRACT (Continue on reverse side if necessary and identify by block number)

An engineering test of the Acoustic Data Capsule (ACODAC) was conducted in the Western Gulf of Mexico on 27 April 1979. In addition, bottom loss data were collected.

These data were reduced using ARL:UT's multipath processing system. Calculated bottom loss increased with frequency and bottom grazing angle, ranging from approximately 1 dB to 6 dB. —> cont.

DD FORM 1 JAN 73 1473 EDITION OF 1 NOV 65 IS OBSOLETE

UNCLASSIFIED

SECURITY CLASSIFICATION OF THIS PAGE (When Data Entered)

Using available geoacoustic data and a bottom loss model, theoretical bottom losses were generated. A good match between actual and theoretical values was obtained. Thus, a relatively accurate geoacoustic model of the Western Gulf of Mexico was derived.

TABLE OF CONTENTS

LIST OF FIGURES

LIST OF TABLES

CHAPTER 1
INTRODUCTION

The Gulf of Mexico Wet Test exercise was conducted on 27 April 1979 in the area of the Mexican Basin shown in Fig. 1-1. The primary objective of the exercise was an engineering test of the Acoustic Data Capsule (ACODAC) system's ability to monitor ambient noise. In addition, signals from a series of SUS were recorded. The purpose of that series was to obtain information about the geoacoustic properties of the bottom in the region. The SUS source track, shown in Fig.1-1, was a north-to-south line approximately 45 km long.

This region of the Gulf where the test was conducted has a relatively level, smooth bottom with a very thick sediment (1000 m thick). Geoacoustic properties of the bottom in the region as derived from available literature are presented in Chapter 2. The sound speed profile is illustrated in Figs. 1-2. Due to the bottom limited characteristic of the region, acoustic propagation from sources at a depth of 91 m is mainly via paths that reflect from and refract through the bottom. Thus, a thorough analysis of acoustic propagation in the area requires the quantification of the bottom sediment acoustic parameters.

The ACODAC system consisted of 12 hydrophones ranging in depth from 3200 to 530 m. The ocean depth in the exercise region is approximately 3400 m. The SUS were detonated at depths of 91 and 244 m. Due to the system electronic setup, only the hydrophone at 2290 m recorded data of sufficient quality to derive propagation loss. There were, however, sufficient data to adequately describe acoustic propagation in the test region.

The analysis was begun using the ARL:UT multipath processing system detailed in Ref. 1. The bottom loss versus bottom angle data described in Chapter 3 are the main data products of this system. Chapter 4 explains the bottom loss

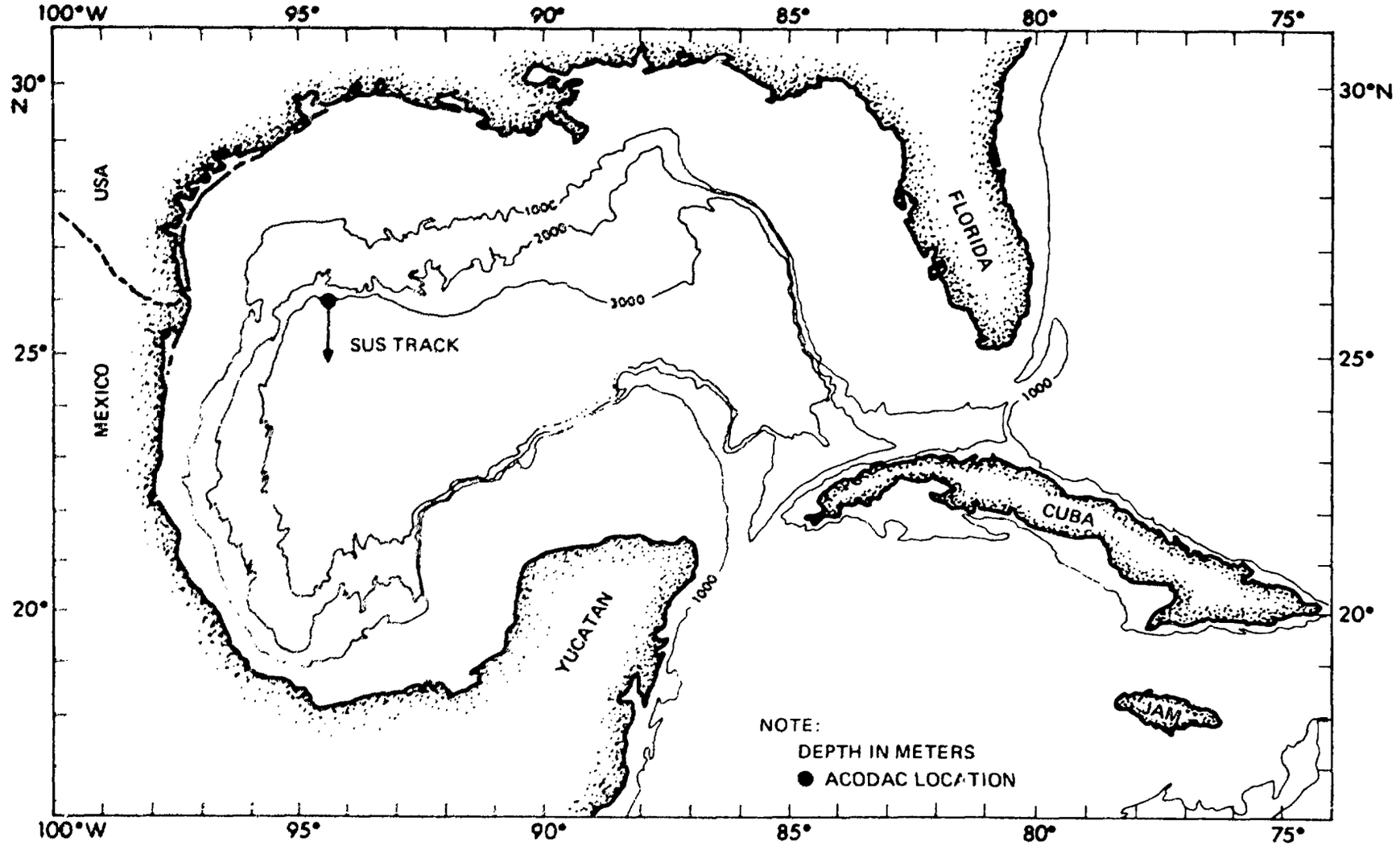

ARL UT
AS-81-683
MMH - GA
7-29-81

FIGURE 1-1
LOCATION OF THE WET TEST SITE AND SUS TRACK

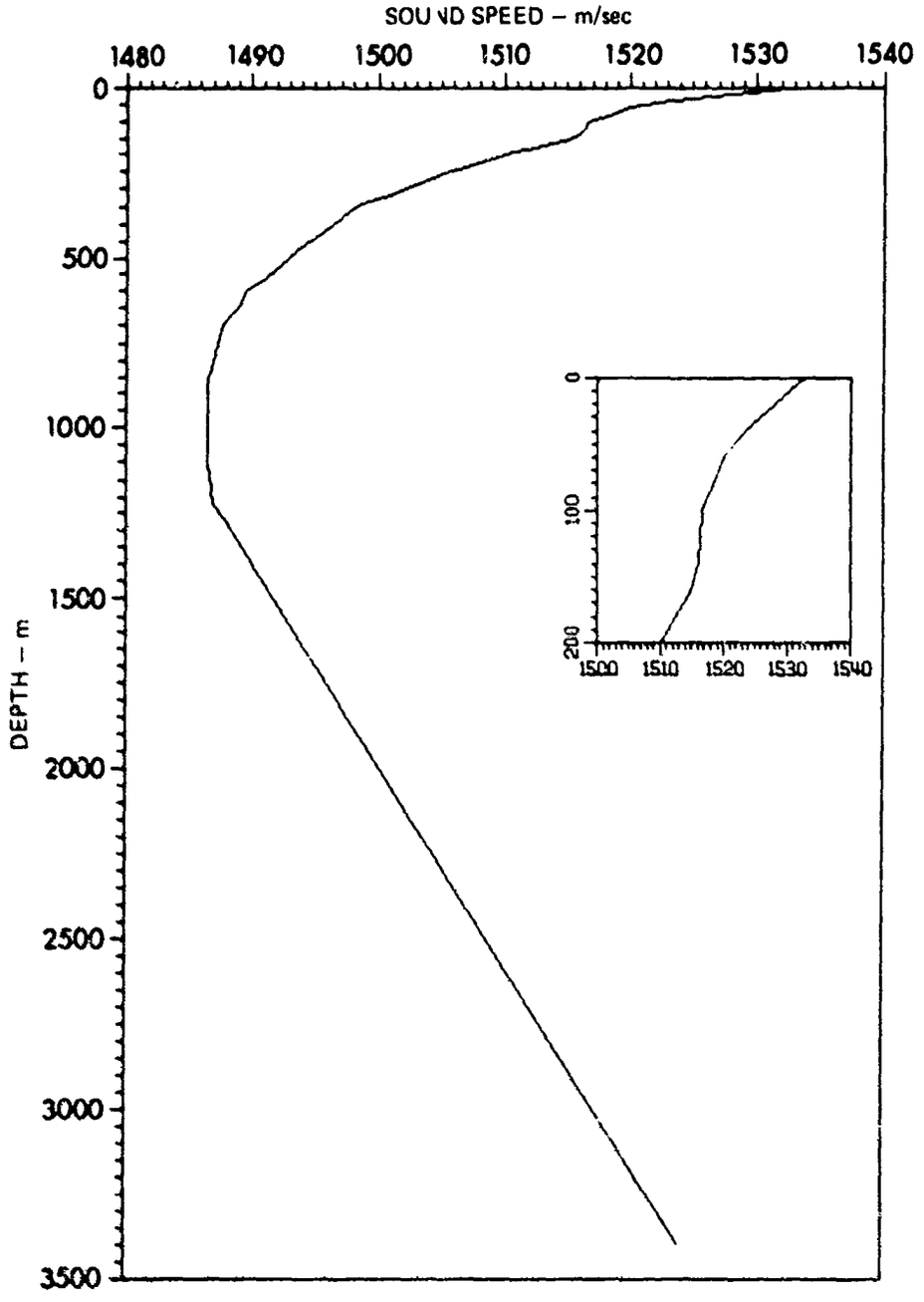

FIGURE 1-2
SOUND SPEED PROFILE FOR WET TEST EXERCISE AREA

ARL:UT
AS-81-1109
MWH · GA
8 · 25 · 81

results in terms of ocean bottom (geoacoustic) models. These geoacoustic models predict signal paths and attenuation using sediment sound speed and density gradients, and the ratio of the compressional wave velocities in the sediment and water at the water-sediment interface. The first two parameters are obtained from geological survey data, presented in Chapter 2, and the ratio was derived from the measured bottom loss data, explained in Chapter 3. The final analytical step compares the measured bottom losses to those obtained from the modeling.

The measurements show the bottom loss to be quite low in the test region. For example, at 32.5° grazing angle, a mean per bounce loss of 2.0 dB occurred at 50 Hz and 4.1 dB at 250 Hz. Bottom losses calculated from the geoacoustic model match quite well with measured data. Thus, a geoacoustic model of the test region has been determined and can accurately predict bottom interactions.

CHAPTER 2
GEOACOUSTIC DATA FOR THE WESTERN GULF OF MEXICO

The data discussed in this report were recorded at a site in the Gulf of Mexico near the boundary of two depositional regions: the Lower Mississippi Fan and the Western Gulf. Figure 2-1 shows the Deep Sea Drilling Project (DSDP) sites in the area,[2,3] and an approximate delineation of depositional regions. Of particular interest in this study are DSDP holes 90, 91, and 92, all near the test area.

Figures 2-2 - 2-4 give information on the DSDP holes. Lithologically, the most significant differences among the DSDP sites are the predominance of pelagic sediment in the first 500 m at hole 90, the presence of sand in the upper 500 m at hole 91, and the shallowness at which claystone occurs at hole 92. The predominance of carbonate ooze in the first few hundred meters at hole 90 is due to a failure of turbidity currents from the east to reach this area, while the upper 180 m of sediment at hole 91 is due primarily to turbidity currents from the Mississippi Fan. The deeper sediments at both holes 90 and 91 appear to be turbidites derived primarily from the north, northwest, and west. However, as shown in Fig. 2-2, sediments down to 500 m are coarser grained at hole 91 than at hole 90 and, in particular, sand is reported at hole 91 but not reported at hole 90.

Hole 92 was drilled on a scarp formed presumably by a salt diapir. The sediments at this site are much more consolidated than sediments at comparable depths on the bathymetrically lower rise area. The greater consolidation suggests that either the sediments at this hole have had a greater depth of burial in the past, or salt diffusion facilitated consolidation.

Figure 2-3 shows the density profiles measured by the DSDP at these sites. These density profiles reflect the lithological differences discussed previously. The

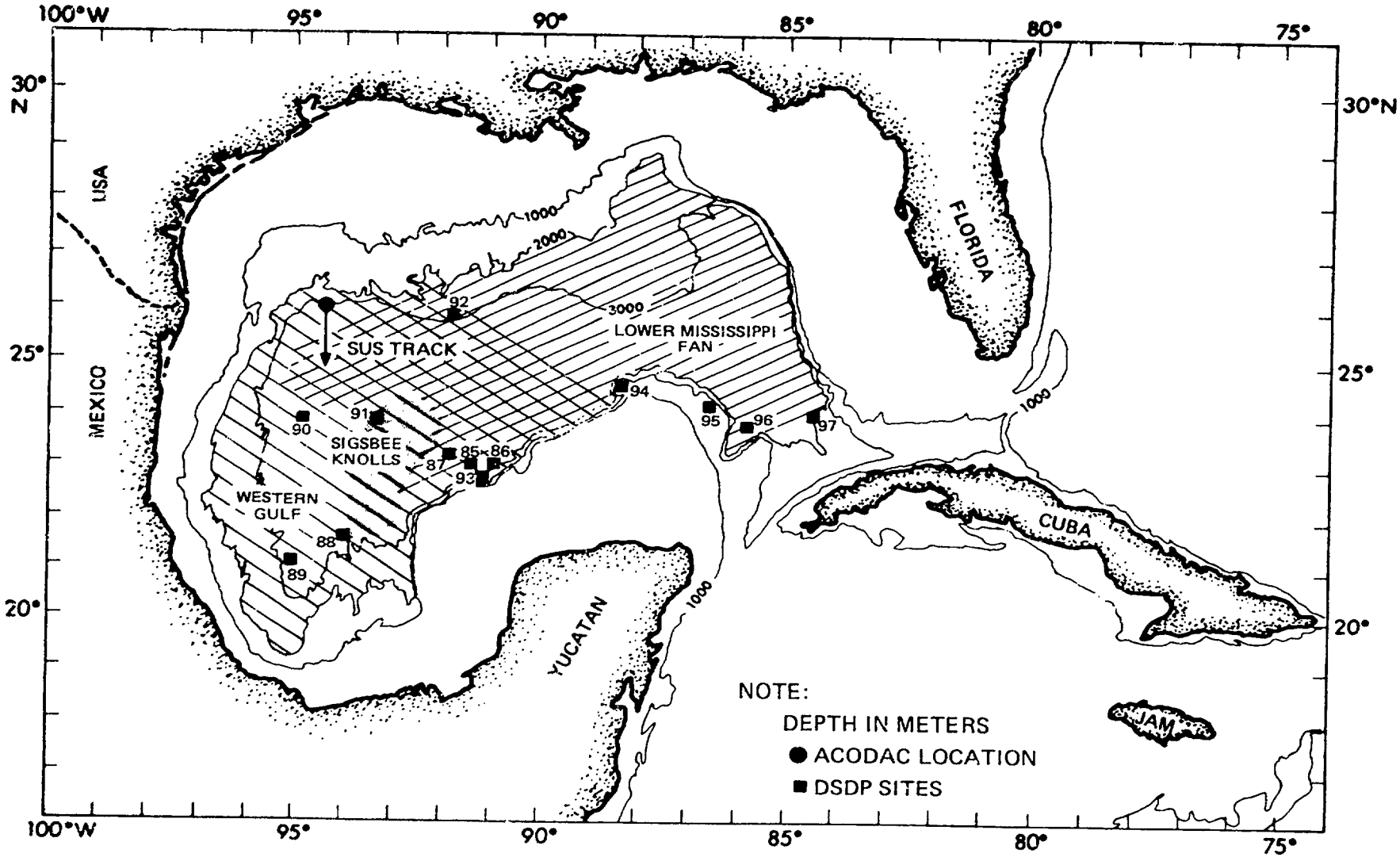

FIGURE 2-1
MAP OF AREA WITH PRELIMINARY DELINEATION OF DEPOSITIONAL REGIONS AND LOCATIONS OF DEEP SEA DRILLING PROJECT (DSDP) HOLES 85-97

ARL-UT
AS-81-939
GDI-GA
8-6-81

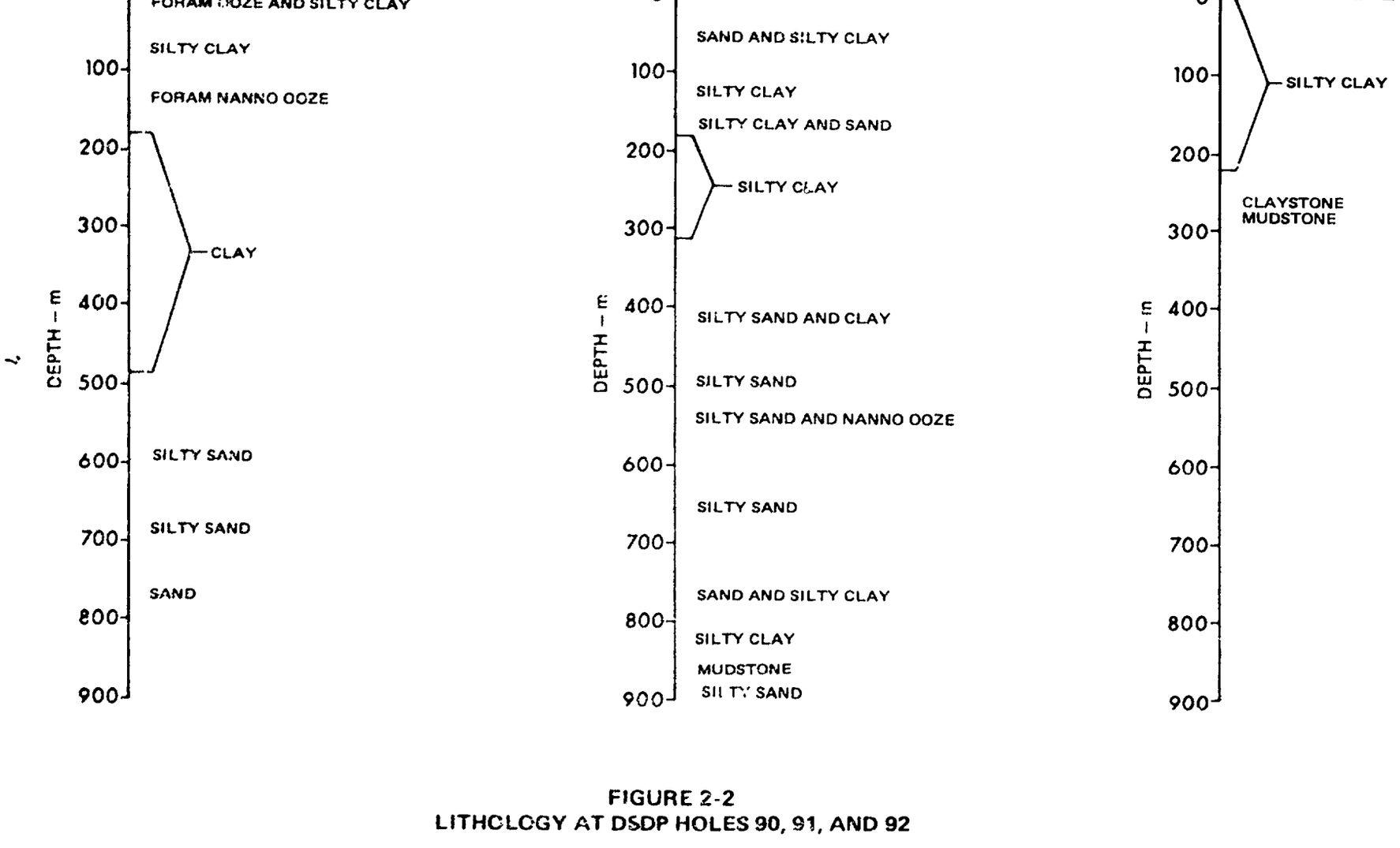

FIGURE 2-2
LITHOLOGY AT DSDP HOLES 90, 91, AND 92

ARL:UT
AS-81-940
GDI-GA
8-6-81

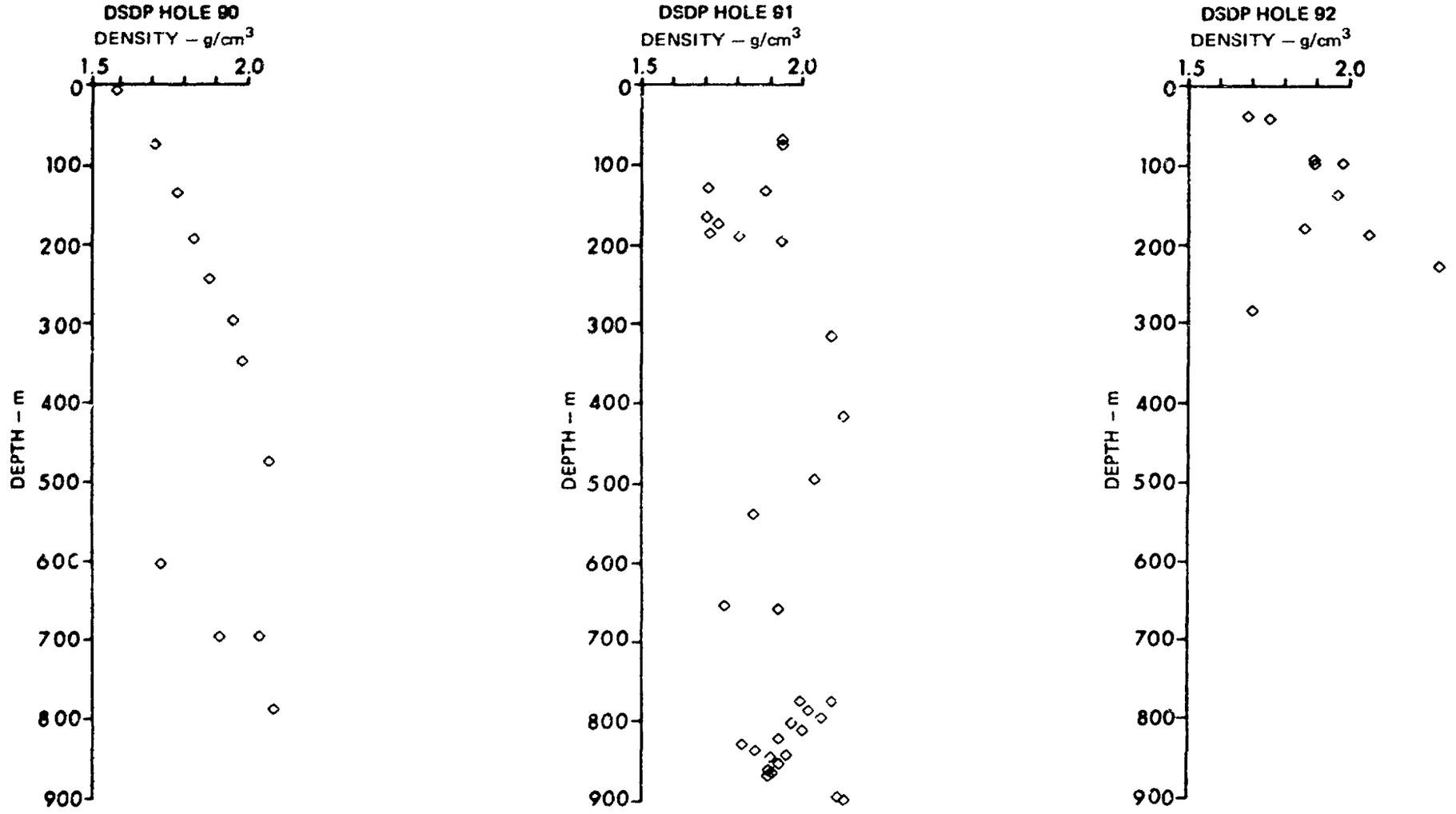

FIGURE 2-3
DENSITY PROFILES FROM DSDP PHYSICAL PROPERTY MEASUREMENTS
AT HOLES 90, 91, AND 92

ARL:UT
AS-81-941
GDI-GA
8-6-81

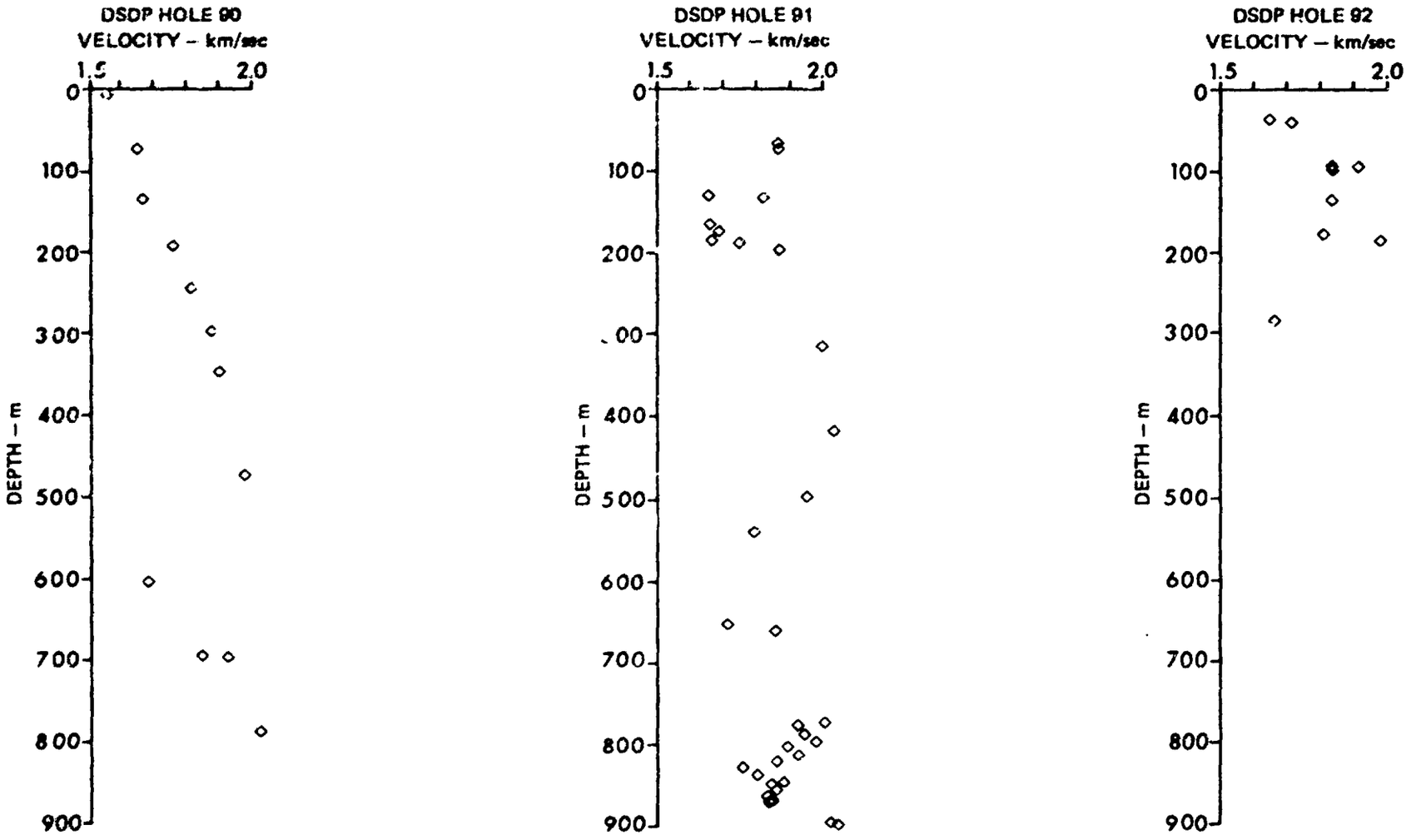

FIGURE 2-4
VELOCITY DATA CALCULATED FROM DENSITY MEASUREMENTS OF THE DSDP USING THE VELOCITY-DENSITY RELATIONSHIPS OF HAMILTON FOR DSDP HOLES 90, 91, AND 92

ARL-UT
AS-81-942
GDI - GA
8-6-81

densities of the turbidites at hole 91 due to the Mississippi Fan are greater and show greater variation with depth than the pelagic sediments at hole 90. Also, the density values of the three holes are largest at hole 92 where the sediments are more consolidated.

Figure 2-4 shows the velocity profiles derived from the density profiles of Fig. 2-3 using the velocity-density relationship of Hamilton.[4] The velocity-density relationship for silt-clays and turbidites was calculated from Hamilton's equation:

$$\rho = 1.135\ Vp - 0.190 \quad .$$

Figure 2-4 shows the large difference between velocity measurements for holes 90, 91, and 92. The gradient at hole 90 is approximately 1 sec^{-1}; at hole 92 it is about 2 sec^{-1}, and at hole 91 it is between 1 sec^{-1} and 2 sec^{-1}. Assuming that the experimental accuracy is the same at each site, one would expect, on the basis of velocity gradients and density contrasts, that bottom loss would be lower at hole 91 than hole 90. This would result from the shorter path lengths at hole 91 due to the higher sound speed gradient and the greater variance of instantaneous impedance with depth. Larger gradients imply smaller radii of curvature of the transmitted paths, and larger variations in impedance lead to more reflections. The relative bottom loss at hole 92 cannot be readily compared to that of holes 90 or 91 since the relief and shape of the scarp at hole 92 will significantly affect bottom loss at this site.

Figure 2-5 shows some velocity profiles found in the literature for the Gulf of Mexico, which provide useful comparisons with those derived from DSDP data. The solid curve is a composite profile derived at the Marine Science Institute (MSI, Galveston, Texas) from multichannel seismic data, shot primarily in the western part of the Gulf.[5] The solid curve with circles is a profile derived by Gregory[6] in a similar region using the percentage of shale in the sediment column to estimate velocity. Finally, the dashed curve was obtained by Matthews[7] from a regression of interval velocities for seismic data obtained in an area of the Gulf of Mexico where the sediments are fine grained and highly consolidated due to rapid deposition.

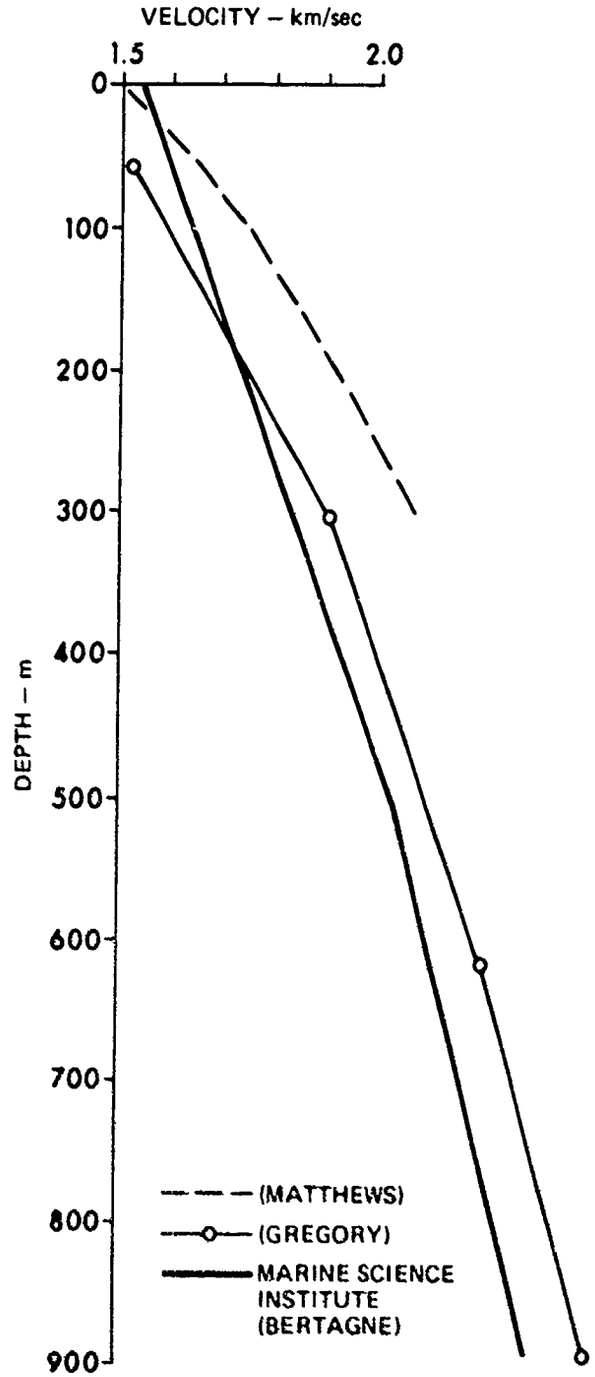

FIGURE 2-5
SOME VELOCITY PROFILES OF THE GULF OF MEXICO FOUND IN THE LITERATURE

ARL:UT
AS-81-943
GDI - GA
8-6-81

Figure 2-6 shows how these profiles compare with the DSDP data. The MSI composite profile agrees very well with the DSDP data at hole 90 down to about 500 m (Fig. 2-6(a)). Below this depth, it is assumed that disturbance of the sample accounts for the unrealistically low DSDP velocities.

Figure 2-6(c) shows that the MSI profile does not agree with the DSDP data at hole 92 and that the Matthews profile underestimates the reported velocity at this site. This is believed due to the anomalously high consolidation of the sediments on the scarp at this site.

Finally, the DSDP measurements at hole 91, shown in Fig. 2-6(b), cannot be matched with the profiles shown in Fig. 2-5. The MSI and Gregory profiles coincide with some of the DSDP data at depths between 100 and 200 m and approximately agree with data points at about 400-500 m, but there is a distinct trend in the data toward sound speeds higher than sound speeds indicated by these profiles. The preliminary explanation of these higher sound speeds is that they are due to a higher coarse grain fraction (in particular sand) at this site than at hole 90. As seen in Fig. 2-2, the lithology at hole 90 is clay and silty clay to a depth of 500 m, whereas the lithology at hole 92 is silty clay, silty sand, and sand. Thus, a reasonable interpretation of the velocities at hole 91 would be a trend similar to that at hole 90 corresponding to the fine grain fraction, superimposed on a discontinuous profile with higher velocities corresponding to sediments with a considerable fraction of sand.

This explanation supports categorization of the Gulf of Mexico into two depositional regions: the Western Gulf, which is characterized by DSDP hole 90 and the MSI velocity profile, and the lower Mississippi Fan, which represents deposition of sediments with a higher coarse grain fraction. DSDP hole 91 seems to be in an overlap area of the two regions.

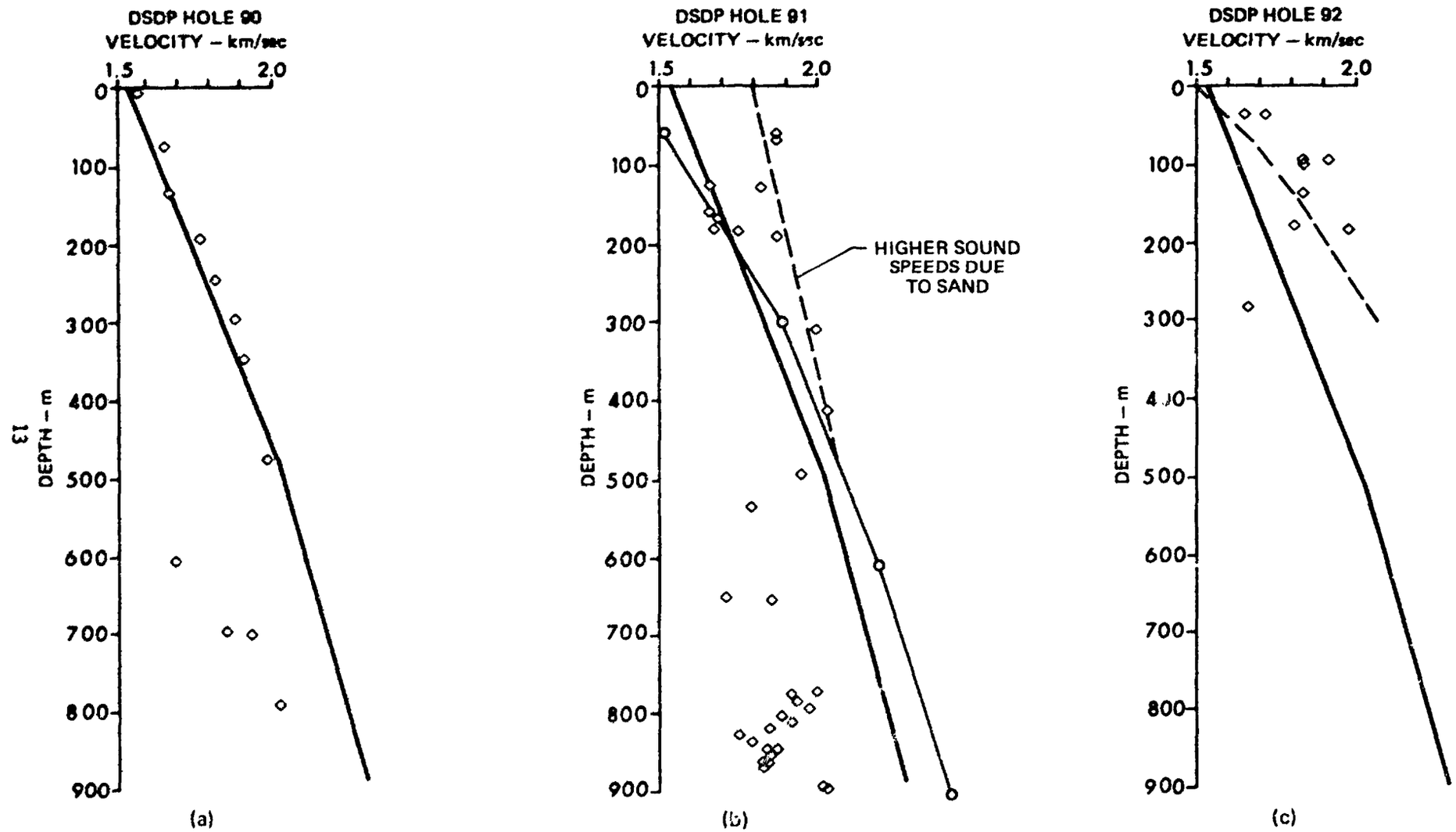

FIGURE 2-6
COMPARISON OF VELOCITY DATA OBTAINED FROM DSDP MEASUREMENTS AND VELOCITY PROFILES FOUND IN THE LITERATURE

ARL:UT
AS-81-344
GDI-GA
8-6-81

The acoustical measurements discussed in this report appear to be in the zone of overlap of these two depositional regions. However, in the absence of other data, the velocity estimate obtained from the MSI composite profile was used in the acoustic analysis. This curve fits the DSDP data at hole 90 very well and appears to be a significant component of the overall velocity profile at hole 91. The sound speeds indicated by the Matthew's profile and DSDP data at hole 92 are probably not applicable to the acoustical measurements discussed in this report, although they are probably suitable for some regions of the Gulf.

Table 2-1 shows sound speeds and densities versus depth obtained from the MSI velocity profile. Densities were computed using the MSI velocity profile and the velocity-density relationships of Hamilton. Note that this sound speed profile shows a slightly "fast" bottom, with a sediment-water speed ratio of 1538/1530 = 1.005. From the analysis of the acoustic bottom interaction data, it was concluded that the ratio should be 1516/1524 = 0.995 (Table 4-1).

TABLE 2-1

VELOCITY AND DENSITY PROFILES

Depth (m)	MSI (m/sec)	Density* (g/cm^3)
0 -	1530	1.0
0 +	1538	1.57
100	1633	1.68
200	1729	1.78
300	1824	1.89
400	1920	1.99
500	2015	2.10
1000	2351	2.23

*Calculated from MSI velocity profile using Hamilton's velocity-density relationships.[4]

CHAPTER 3
BOTTOM LOSS DATA

The processing procedure used to derive the bottom loss data is described in Ref. 1 and consists of three main steps. First, the total propagation loss for each multipath arrival is determined by comparing received energy in the pulse to the standard source level for the SUS. Next, using a coherence ray theory model and assuming a perfectly reflecting bottom, a reference loss for each arrival is calculated. The bottom loss calculated for each arrival is then assumed to be the difference between the reference and measured losses. Measurements are made in standard 1/3 octave bands from 25 Hz to 300 Hz.

The reduced data consisted of 48 SUS detonated at 91 m depth and 47 SUS at 244 m depth. The data used were recorded from a receiver at 2290 m depth.

The bottom loss data were limited to frequencies of 300 Hz or less, the bandwidth of the ACODAC. Exercise geometry restricted the bottom grazing angles of usable signal arrivals to between 7° and 38°. Short range SUS produced arrivals with grazing angles greater than 38°, but these saturated the receiver. The exercise conditions resulted in a problem for arrivals with low grazing angles (7° or less). The receiver was approximately 1110 m above the bottom. The sound speed profile (Figs. 1-2) indicates that bottom refraction can occur for sources deeper than 60 m; these paths also refract at the surface. The 244 m sources have more rays which refract rather than bounce from the surface than the 91 m shots. As a result, for 25 of the 244 m shots, bottom refracted arrivals were received within 0 to 150 msec prior to bottom bounce arrivals. These could not be time resolved, and contaminated bottom loss data below 14°. This situation occurred only four times for the 91 m shots and then disturbed data for bottom angles of less than 7°. Had the receiver been farther from the bottom, this problem would have been lessened.

Figures 3-1 - 3-5 are the per bounce bottom loss curves of five frequencies for the 244 m source. Figures 3-6 - 3-9 contain similar data for the 91 m sources. In these figures, each plotted symbol represents a bottom loss measurement from a single arrival. The plotted number denotes the number of bottom reflections of that arrival.

At 25 Hz and 50 Hz for the 91 m SUS and at 25 Hz for the 244 m SUS, the curves show complex behavior and have negative values over some angular intervals. Those are artifacts that arise from a combination of the acoustic surface interference effect ("Lloyd's mirror effect") and inaccurate source navigation.[1] Research is currently underway to circumvent this problem by estimating arrival angles from the data rather than from calculations based on navigation.[8] These low frequency bottom loss data can be interpreted as meaning that the loss is very low; actual values must be estimated from the higher frequency data, as will be done in Chapter 4.

Curves illustrating the per bounce bottom loss averaged over consecutive 5° bins are presented in Figs. 3-10 (91 m), 3-11 (244 m), and 3-12 (both sources). Note that the bottom loss scale is expanded. Because of the measurement artifact problems, the 25 Hz and 50 Hz data for the 91 m SUS and the 25 Hz data for the 244 m SUS are excluded. Comparing data from the two source depths (Figs. 3-10 and 3-11), one sees a close agreement of the estimates.

For both sources, bottom loss increases with frequency and bottom grazing angle. Mean bottom loss per bounce ranged from near 1 dB at 7° to approximately 2.5 dB at 38° for 50 Hz. Losses at 250 Hz rose from 4 dB at 7° to 5.7 dB at 38°.

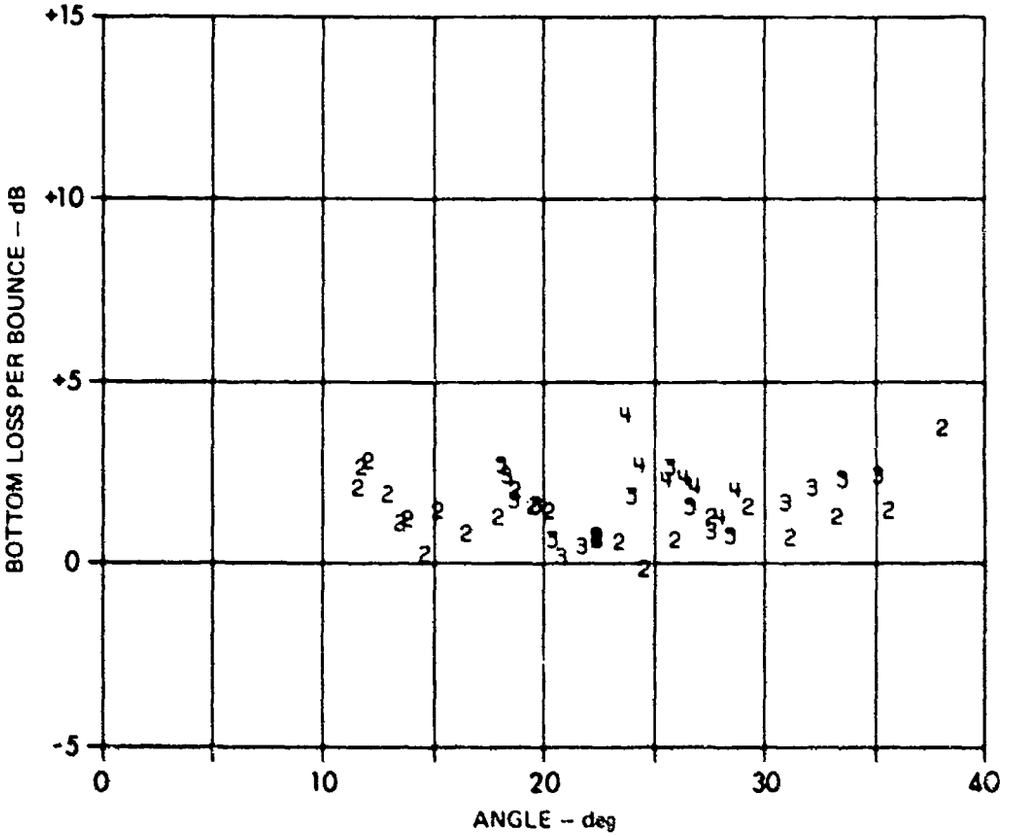

FIGURE 3-1
50 Hz BOTTOM LOSS PER BOUNCE versus GRAZING ANGLE
FOR A 244 m SOURCE AND A 2290 m RECEIVER

ARL-UT
AS-81-1110
MWH-GA
8-25-81

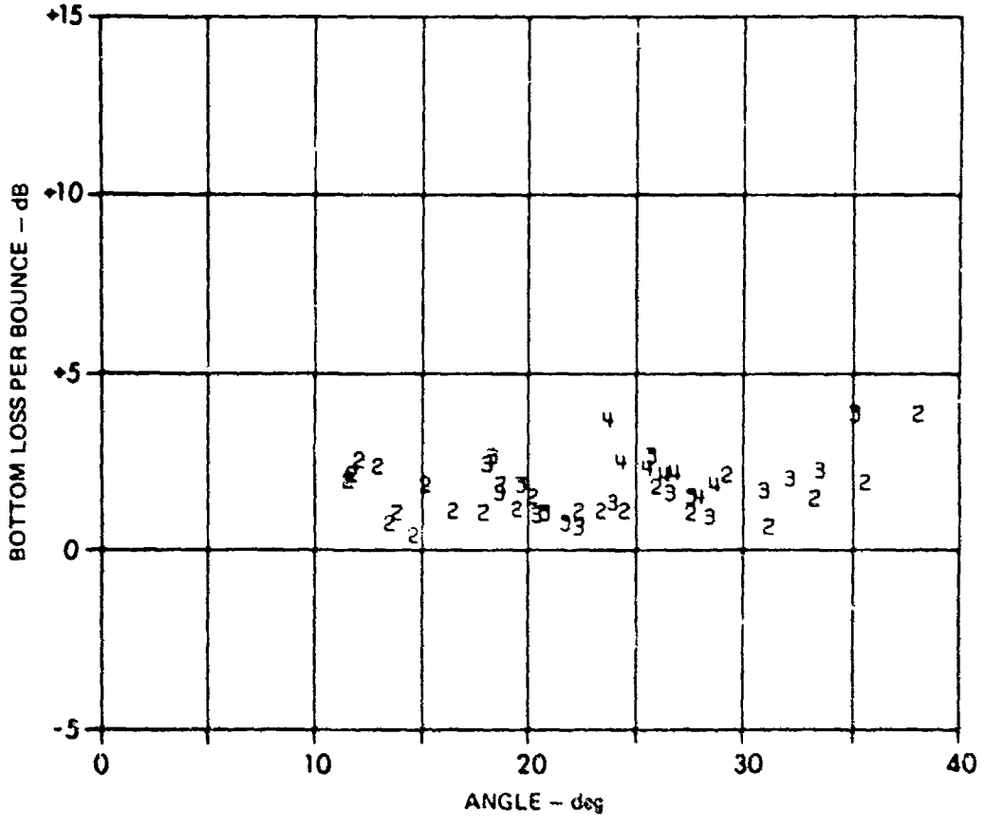

FIGURE 3-2
100 Hz BOTTOM LOSS PER BOUNCE versus GRAZING ANGLE
FOR A 244 m SOURCE AND A 2290 m RECEIVER

ARL-UT
AS-81-1111
MNH - GA
8-25-81

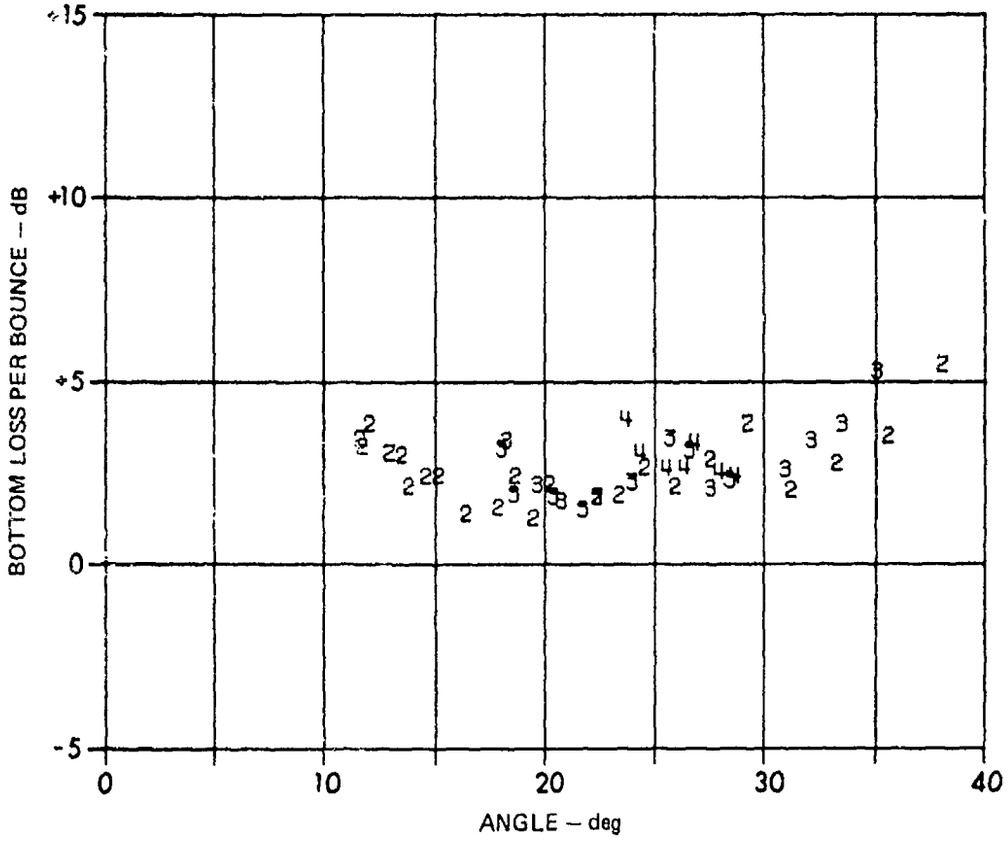

FIGURE 3-3
160 Hz BOTTOM LOSS PER BOUNCE versus GRAZING ANGLE FOR A 244 m SOURCE AND A 2290 m RECEIVER

ARL·UT
AS-81-1112
MWH · GA
8 · 25 · 81

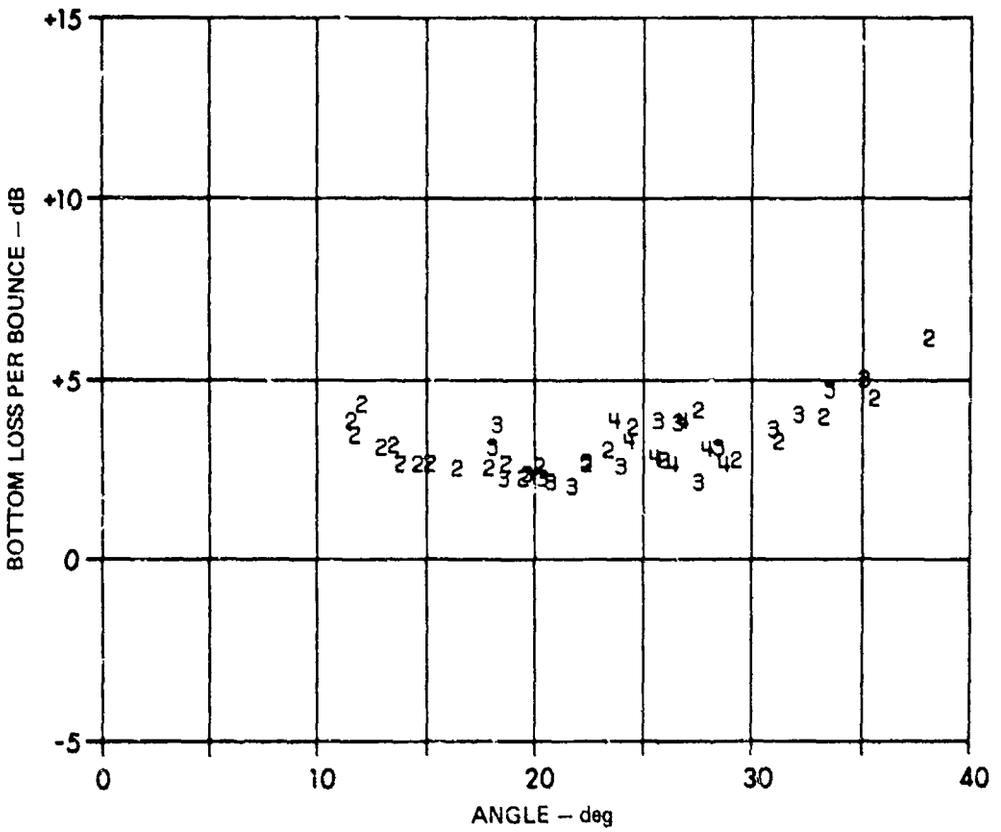

FIGURE 3-4
200 Hz BOTTOM LOSS PER BOUNCE versus GRAZING ANGLE FOR A 244 m SOURCE AND A 2290 m RECEIVER

ARL:UT
AS-81-1113
MWH - GA
8 - 25 - 81

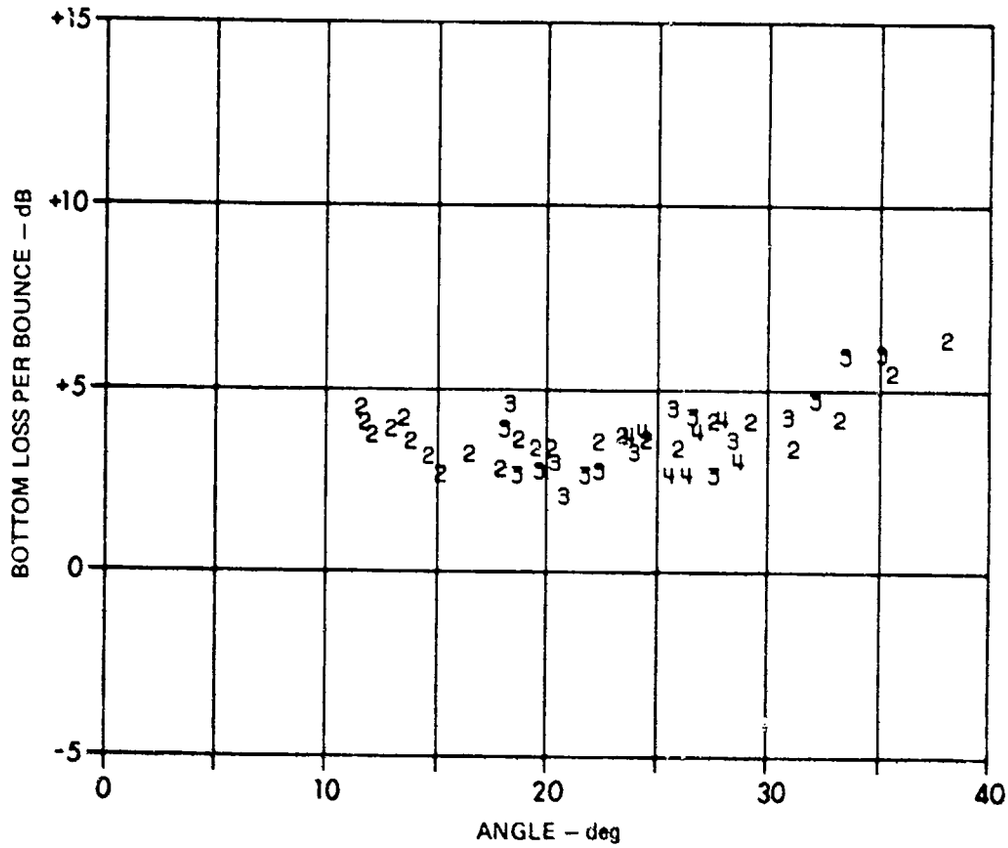

FIGURE 3-5
250 Hz BOTTOM LOSS PER BOUNCE versus GRAZING ANGLE
FOR A 244 m SOURCE AND A 2290 m RECEIVER

ARL:UT
AS-81-1114
MWH - GA
8 - 25 - 81

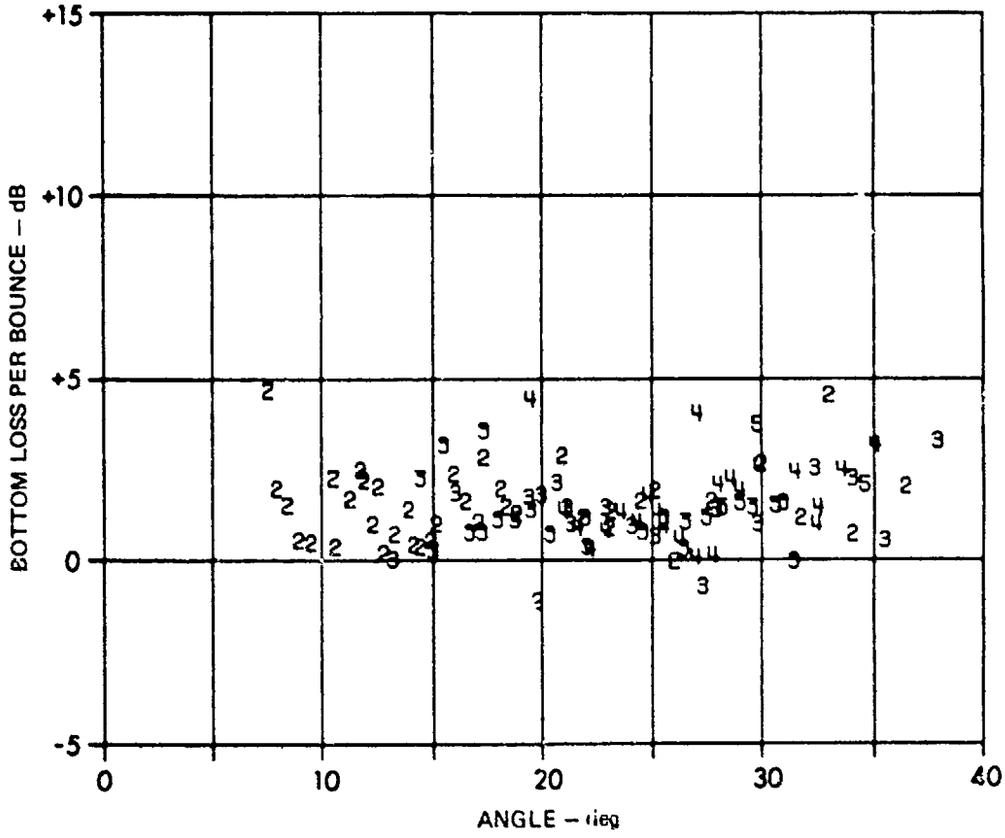

FIGURE 3-6
100 Hz BOTTOM LOSS PER BOUNCE versus GRAZING ANGLE
FOR A 91 m SOURCE AND A 2290 m RECEIVER

ARL:UT
AS-81-1115
MWH · GA
8 · 25 · 81

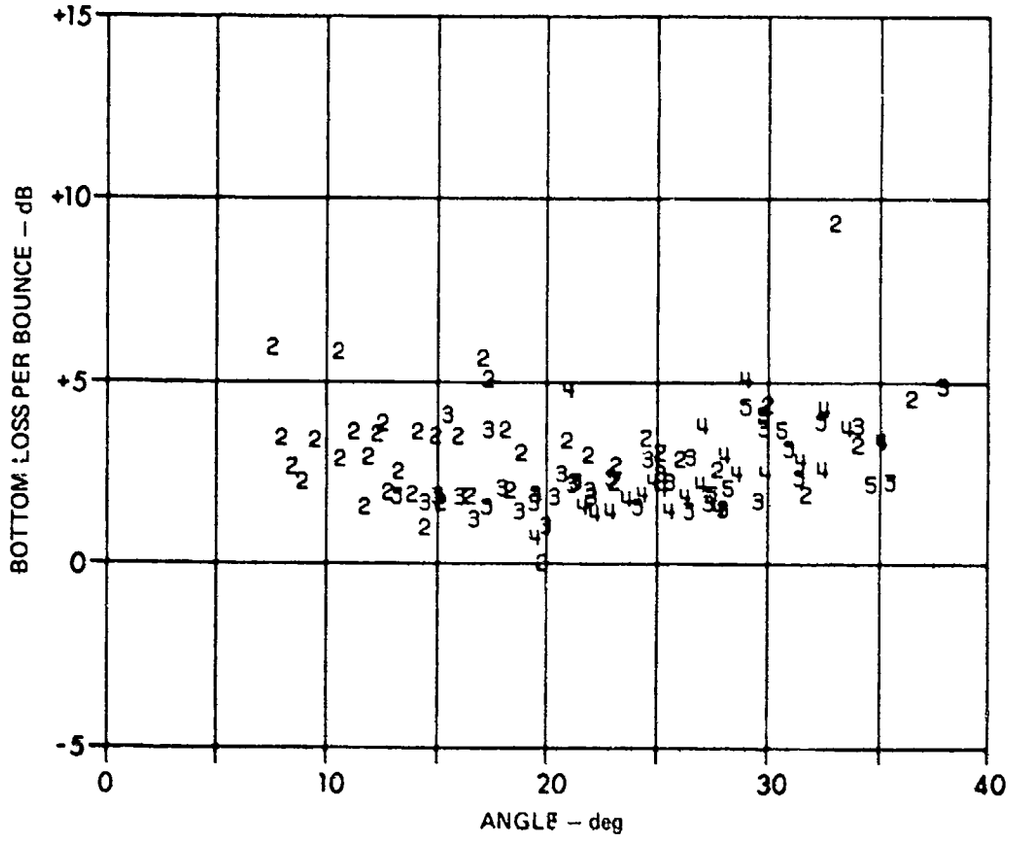

FIGURE 3-7
160 Hz BOTTOM LOSS PER BOUNCE versus GRAZING ANGLE
FOR a 91 m SOURCE AND A 2290 m RECEIVER

ARL-UT
AS-81-1116
MWH - GA
8 - 25 - 81

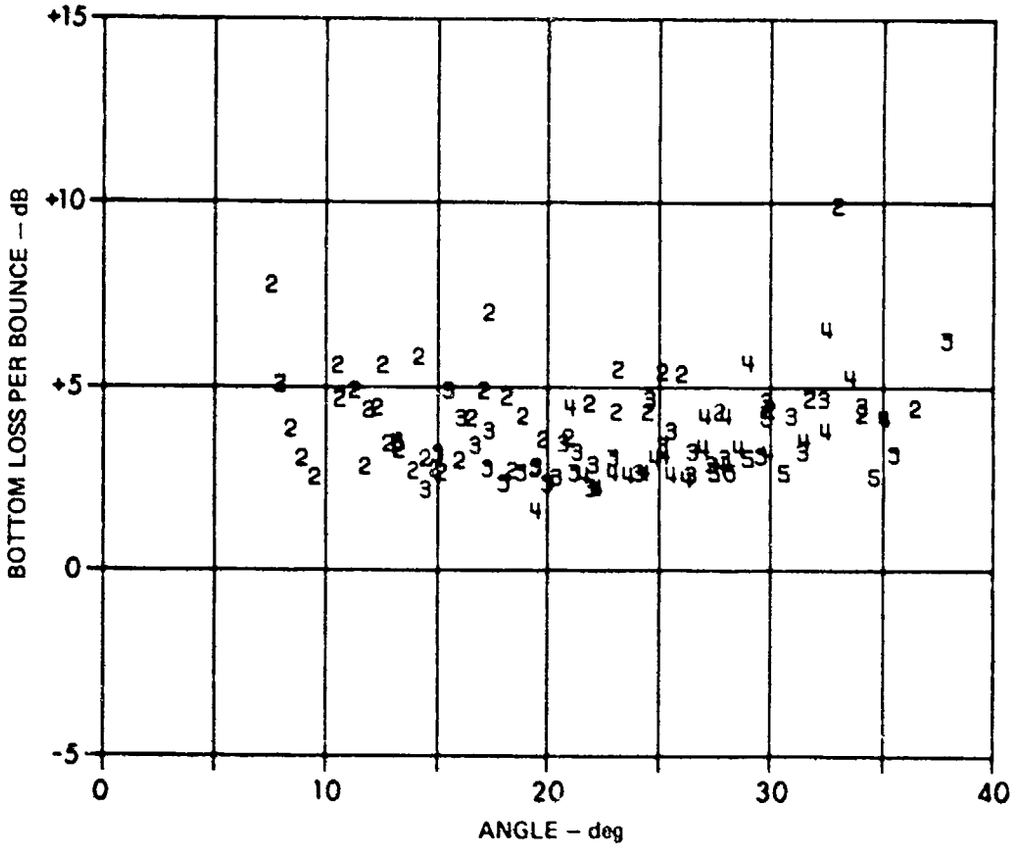

FIGURE 3-8
200 Hz BOTTOM LOSS PER BOUNCE versus GRAZING ANGLE FOR A 91 m SOURCE AND A 2290 m RECEIVER

ARL:UT
AS-81-1117
MWH - GA
8 - 25 - 81

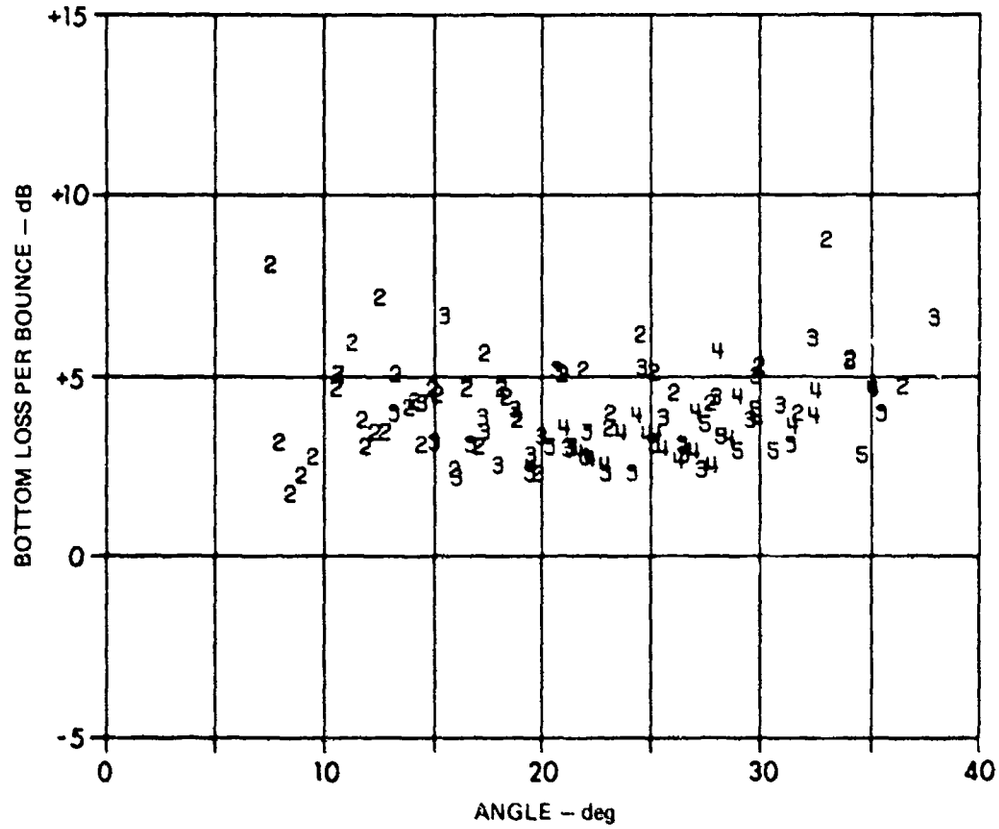

FIGURE 3-9
250 Hz BOTTOM LOSS PER BOUNCE versus GRAZING ANGLE FOR A 91 m SOURCE AND A 2290 m RECEIVER

ARL:UT
AS-81-1118
MWH - GA
8 - 25 - 81

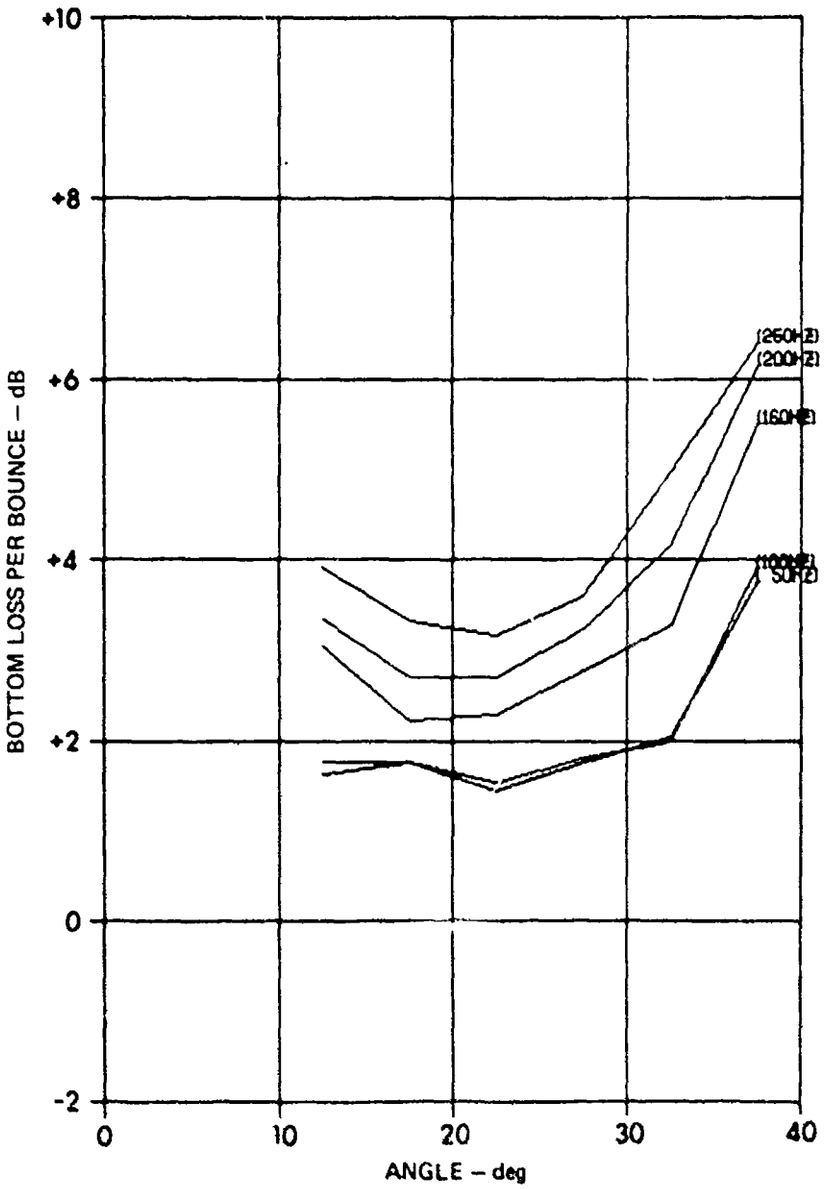

FIGURE 3-10
AVERAGED BOTTOM LOSS PER BOUNCE versus GRAZING ANGLE FOR A 244 m SOURCE AND A 2290 m RECEIVER

ARL:UT
AS-81-1119
MWH - GA
8 - 25 - 81

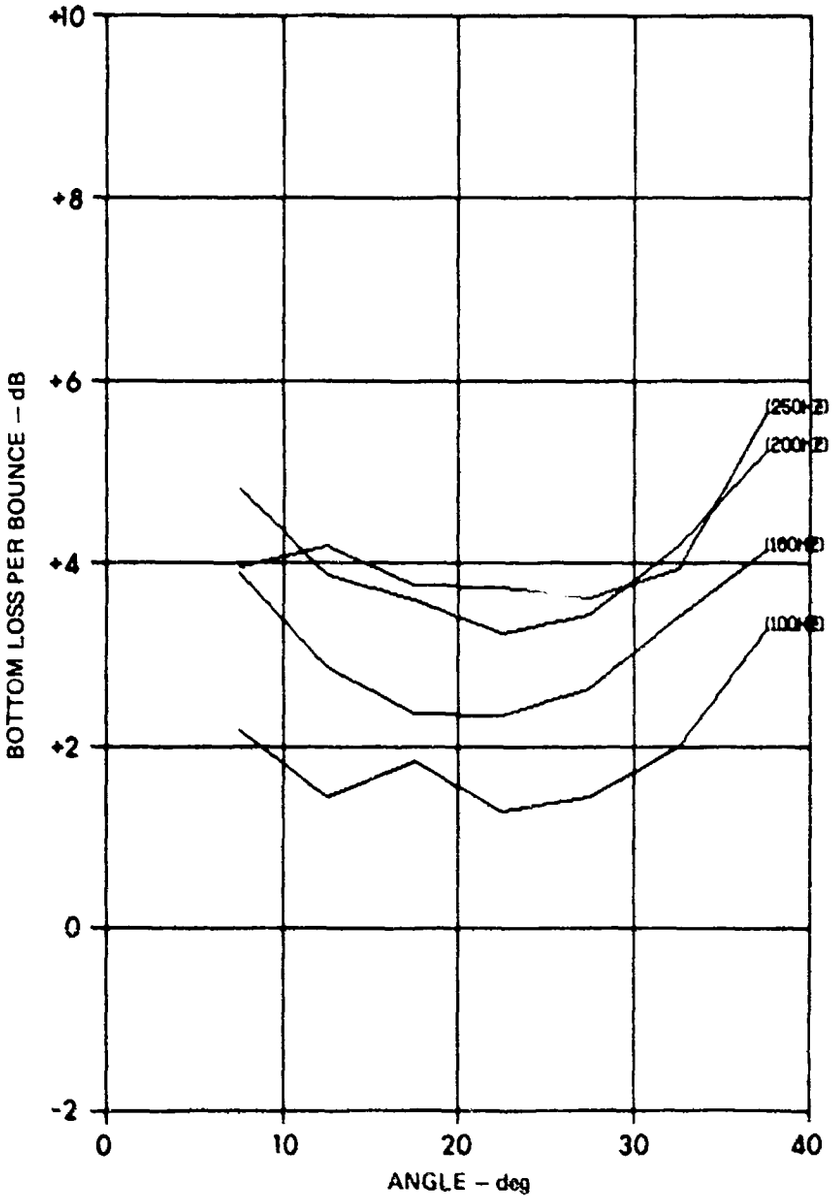

FIGURE 3-11
AVERAGED BOTTOM LOSS PER BOUNCE versus GRAZING ANGLE FOR A 91 m SOURCE AND A 2290 m RECEIVER

ARL:UT
AS-81-1120
MWH · GA
8 · 25 · 81

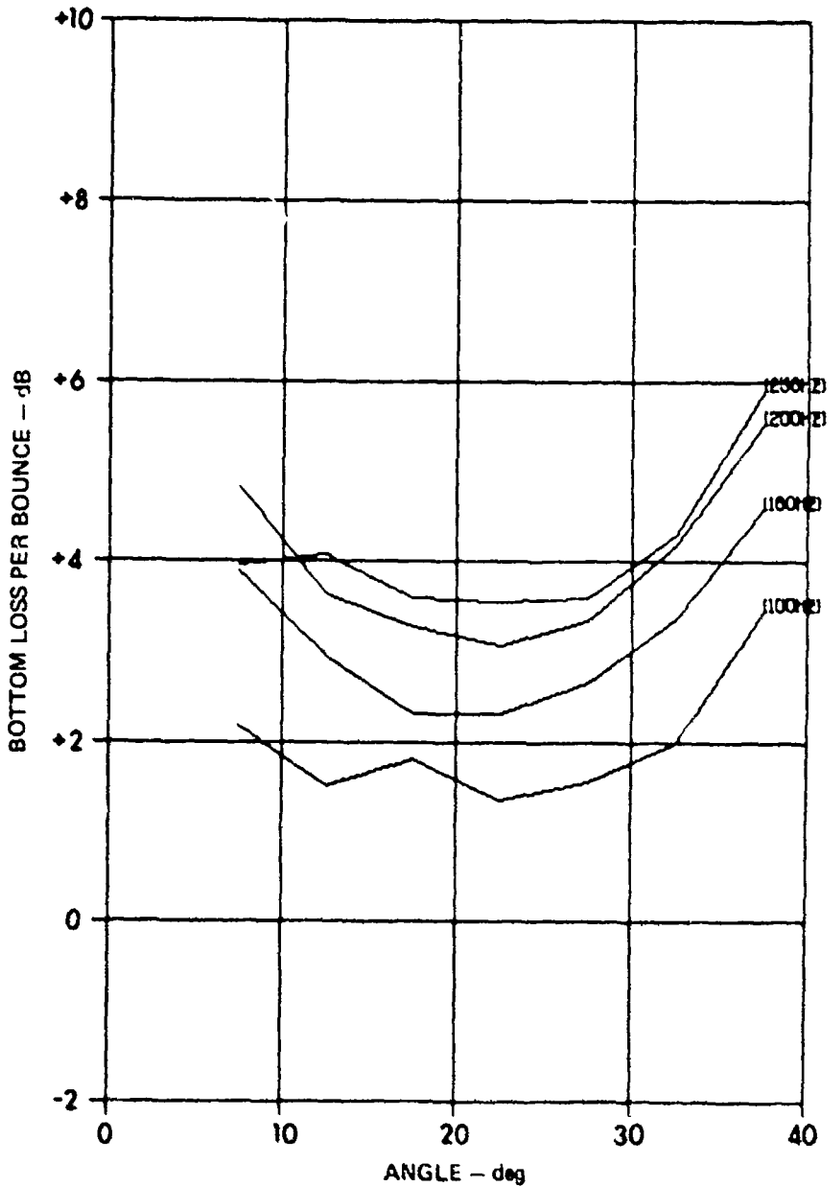

FIGURE 3-12
AVERAGED BOTTOM LOSS PER BOUNCE versus GRAZING ANGLE FOR BOTH SOURCE DEPTHS AND A 2290 m RECEIVER

ARL:UT
AS-81-1121
MWH - GA
8 - 25 - 81

CHAPTER 4
GEOACOUSTIC MODEL OF WET TEST EXERCISE REGION

The second analysis objective was to determine how well the bottom loss measurements could be duplicated by theoretical models. This bottom interaction modeling is based on geoacoustical structure of the ocean bottom, in particular, that constructed by Hamilton.[9] The model describes the bottom as a multilayered, fluid sediment on top of a solid, non-layered basement. Each layer is defined by a depth function of the geoacoustic parameters. This framework was used by Mitchell and Lemmon[10] to develop a ray theory model of acoustic interaction with the ocean bottom. The following analysis is based upon this model. The parameters consist of the velocity and density profiles, attenuation profile, and the ratio of the sediment-to-water sound speeds (c_s/c_w) at the water-sediment interface.

As described in Chapter 2, an initial sound speed profile was obtained from analysis of archival data. Density data were derived from the velocity using Hamilton's density-velocity relationships.[4] Then, an iterative series of bottom loss calculations and comparisons with data, followed by modifications to the geoacoustic model, were conducted. The objective here was to refine the c_s/c_w ratio and to determine the attenuation profile.

The c_s/c_w ratio was determined from the measured bottom loss data. This parameter strongly affects bottom loss at low grazing angles. Therefore, preliminary modeling results were compared to the measured loss to determine the best ratio. The value of 0.995 was selected and the velocity gradients, given in Chapter 2, were then used to calculate the velocity profile shown in Table 4-1.

To obtain the attenuation profile, the inversion technique of Ref. 9 was used. The resulting profile is shown in Fig. 4-1, and is tabulated in Table 4-1. Also shown

TABLE 4-1

GEOACOUSTIC PARAMETERS FOR THE SEDIMENT IN THE WET TEST EXERCISE AREA

	Depth (m)	Velocity (m/sec)	Compressional Wave Attenuation (dB/m-kHz)	Density $(g/cm)^3$
Bottom Water		1524		1.04
Sediment	0	1516	0.033	1.57
	50	1563	0.015	1.63
	100	1611	0.008	1.69
	200	1706	0.008	1.78
	300	1801	0.010	1.89
	400	1896	0.012	1.99
	500	1991	(0.012)*	(2.10)*
	1000	2327	(0.012)*	(2.23)*

*Values in parenthesis were extrapolated.

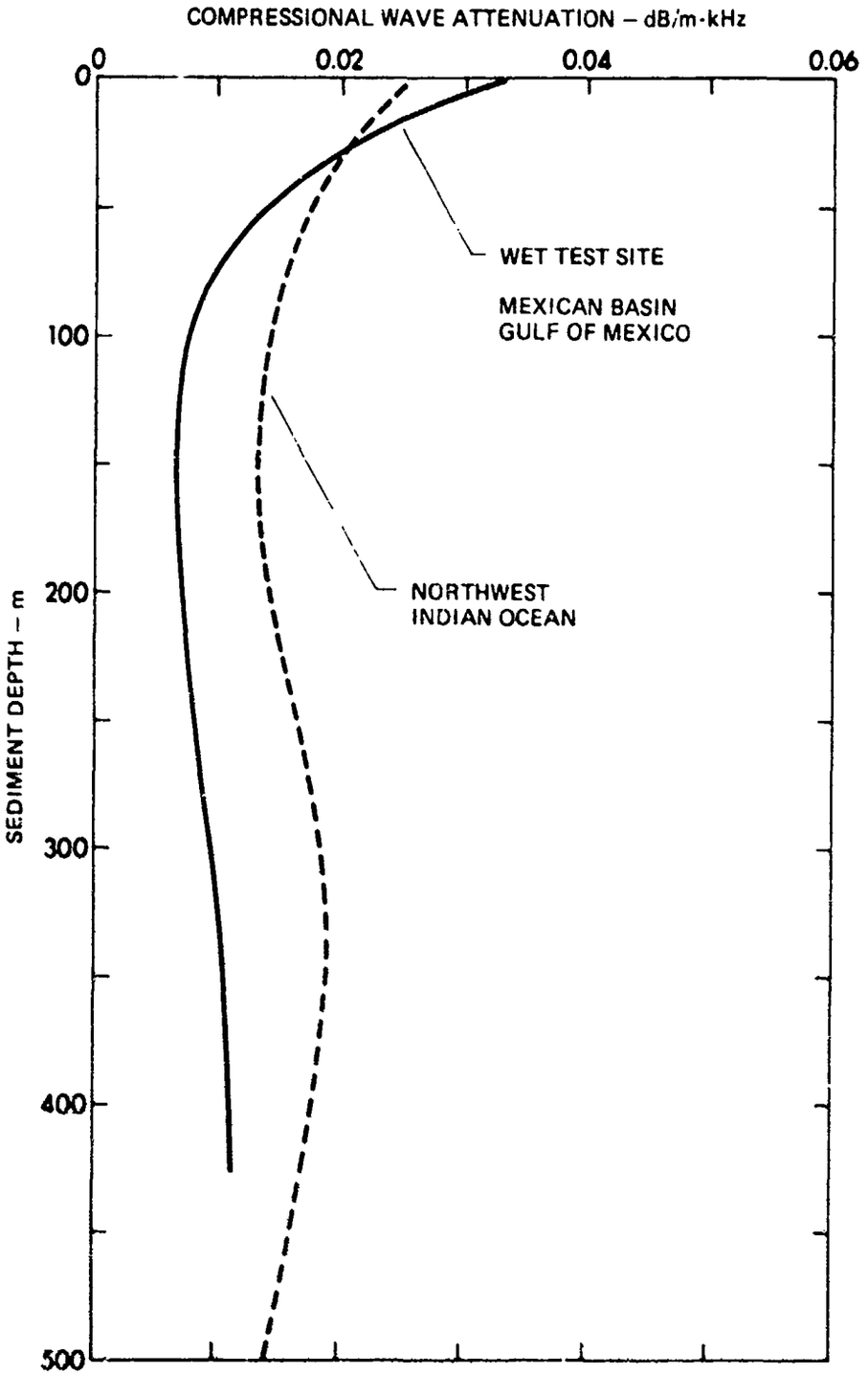

FIGURE 4-1
COMPARISON OF ATTENUATION PROFILES FOR THE WET TEST SITE AND THE NORTHWEST INDIAN OCEAN

ARL:UT
AS-81-884
MWH - GA
7 - 29 - 81

in Fig. 4-1 is the attenuation profile derived for thick sediment regions of the Northwest Indian Ocean.[11] The attenuation data from the Mexican Basin Wet Test site closely match those labeled "M" (medium) from the Indian Ocean. As reported in Ref. 11, that region is known to have a silty clay bottom of terrigeneous origin with turbidite layering. A similar structure should be expected for the Wet Test region as discussed in Chapter 2.

Figures 4-2 - 4-6 compare the calculated and combined measured bottom loss. The figures illustrate very good agreement. Both measured and calculated values are averaged over 1/3 octave bands. Table 4-2 contains the calculated bottom losses for five frequencies and for grazing angles from 8° to 36°.

This close match is important, as it allows extrapolations to the frequency and angle limits imposed by the measurement system.

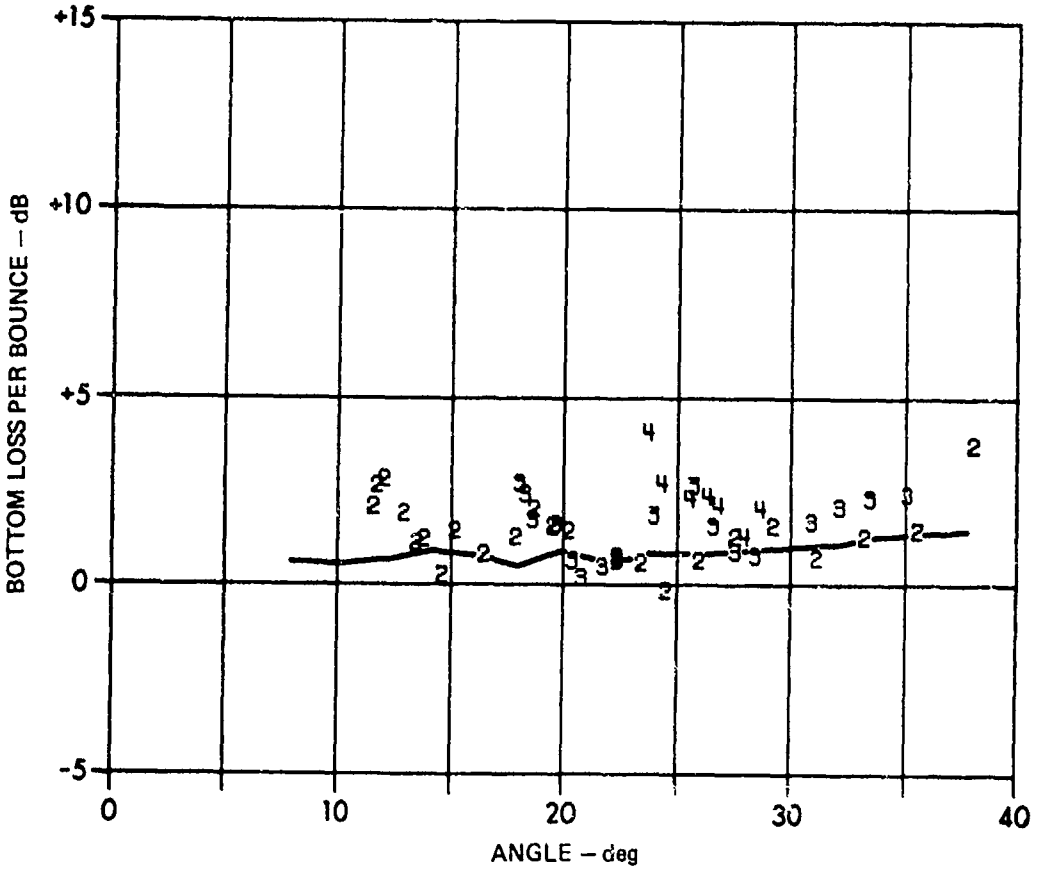

FIGURE 4-2
COMPARISON OF CALCULATED (SOLID LINE) AND MEASURED (NUMBERS)
50 Hz BOTTOM LOSS PER BOUNCE versus GRAZING ANGLE

ARL:UT
AS-81-685
MWH - GA
7 - 29 - 81

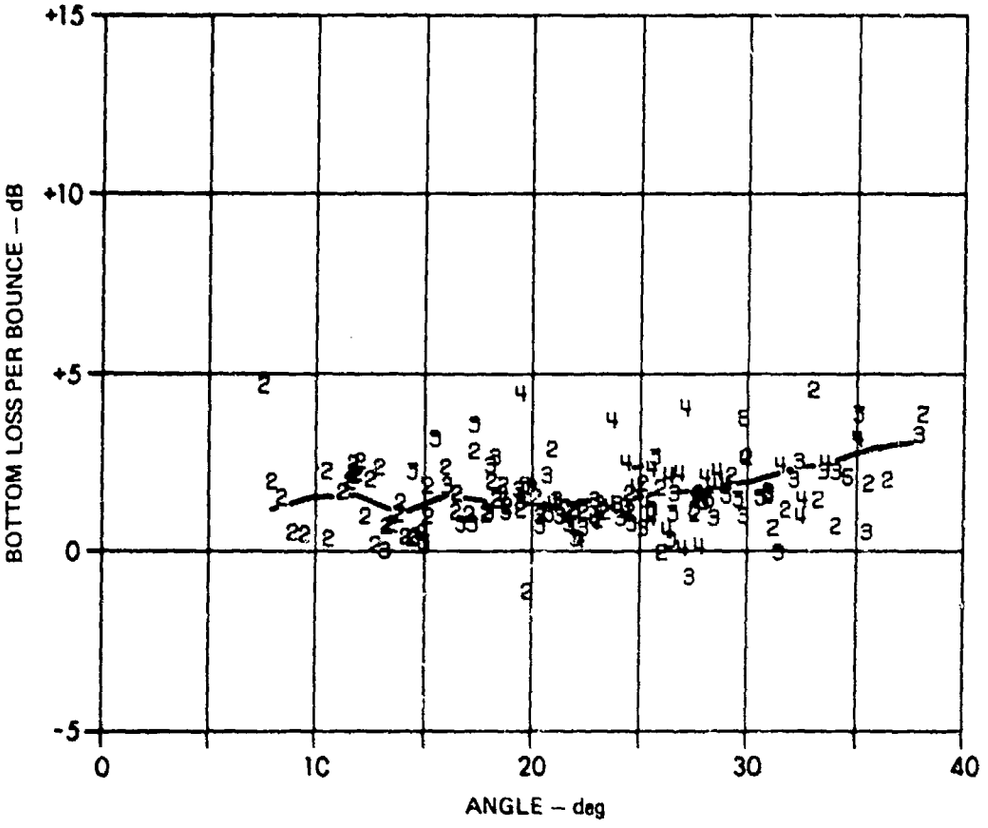

FIGURE 4-3
COMPARISON OF CALCULATED (SOLID LINE) AND MEASURED (NUMBERS)
100 Hz BOTTOM LOSS PER BOUNCE versus GRAZING ANGLE

ARL:UT
AS-81-886
MWH · GA
7 · 29 · 81

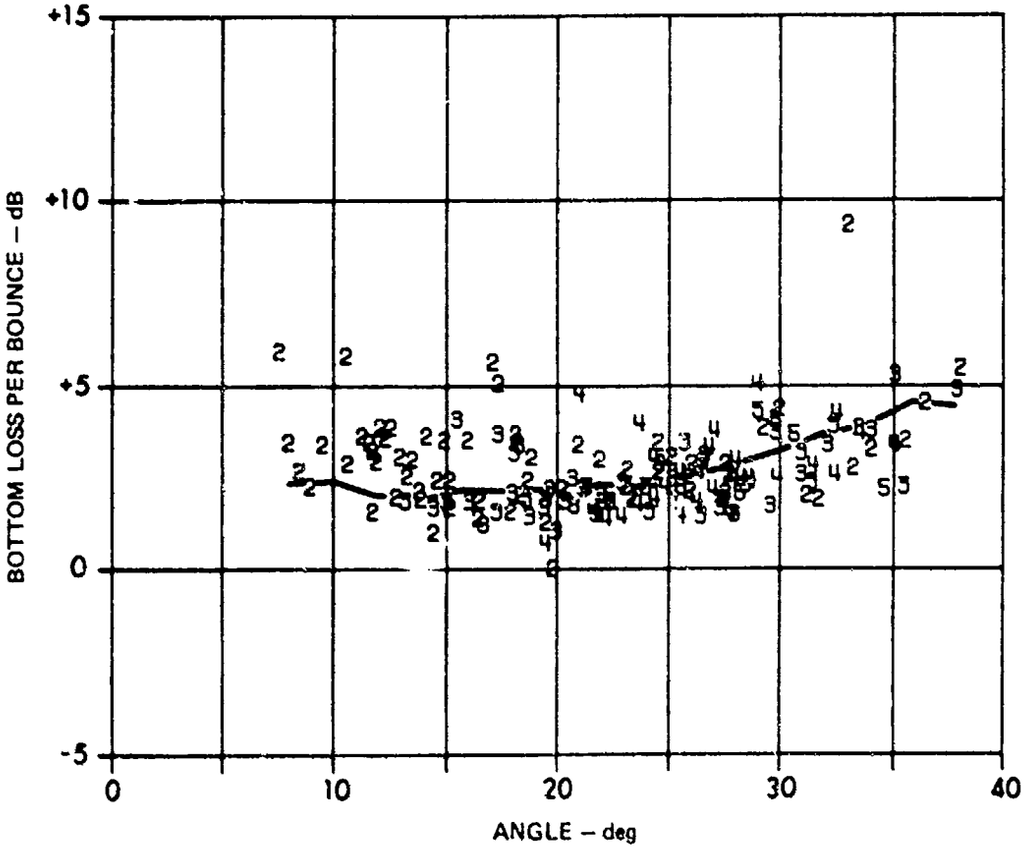

FIGURE 4-4
COMPARISON OF CALCULATED (SOLID LINE) AND MEASURED (NUMBERS) 165 Hz BOTTOM LOSS PER BOUNCE versus GRAZING ANGLE

ARL:UT
AS-81-887
MWH - GA
7 - 29 - 81

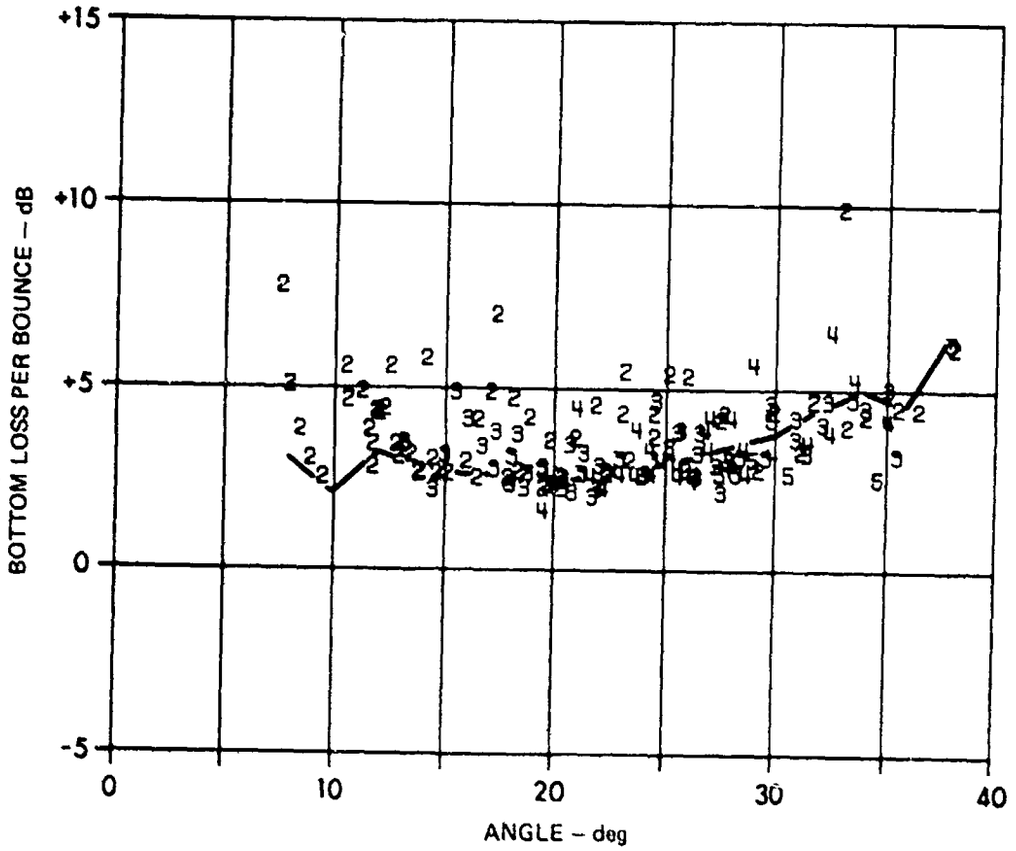

FIGURE 4-5
COMPARISON OF CALCULATED (SOLID LINE) AND MEASURED (NUMBERS)
200 Hz BOTTOM LOSS PER BOUNCE versus GRAZING ANGLE

ARL:UT
AS-81-888
MWH - GA
7 - 29 - 81

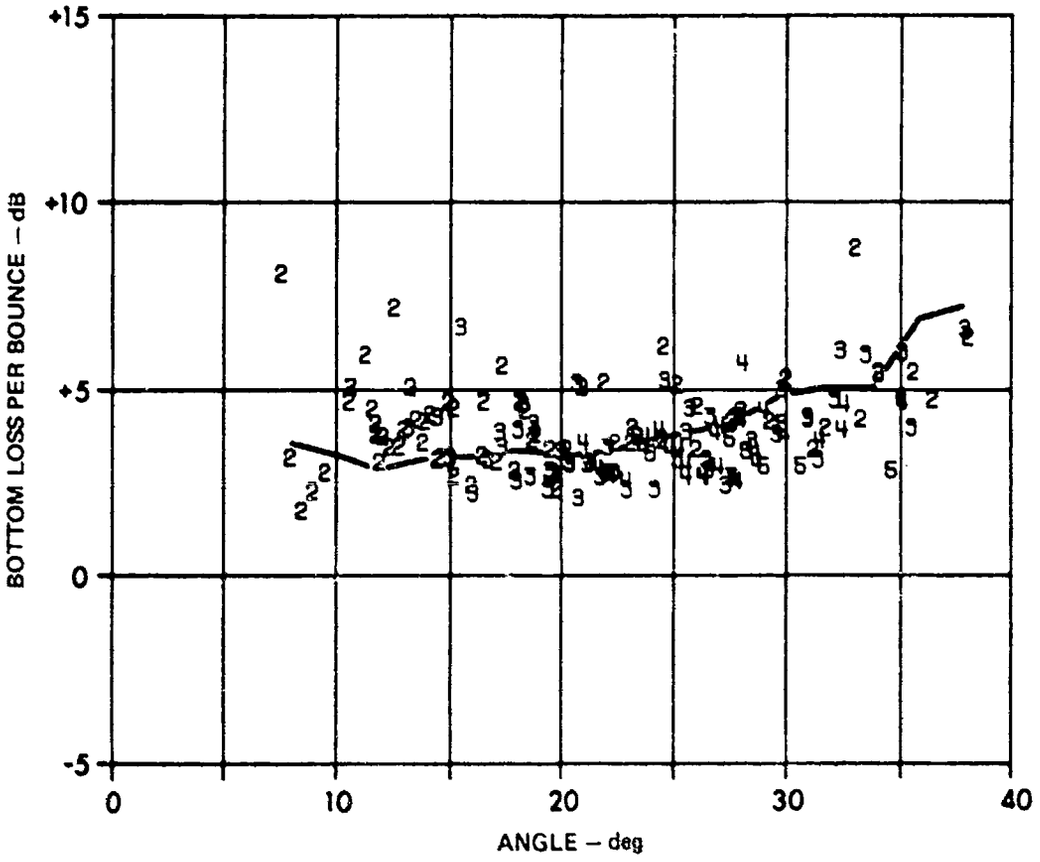

FIGURE 4-6
COMPARISON OF CALCULATED (SOLID LINE) AND MEASURED (NUMBERS)
250 Hz BOTTOM LOSS PER BOUNCE versus GRAZING ANGLE

ARL:UT
AS-81-889
MWH - GA
7 - 29 - 81

TABLE 4-2

BOTTOM LOSSES CALCULATED BY A GEOACOUSTIC MODEL OF THE MEXICAN BASIN OF THE GULF OF MEXICO

Grazing Angle (deg)	Bottom Loss (dB) Frequency (Hz)				
	50	100	160	200	250
8	0.5	1.1	2.2	3.1	3.5
12	0.6	1.5	1.9	3.2	2.8
16	0.7	1.3	2.1	2.6	3.1
20	0.8	1.3	2.1	2.5	3.2
24	0.7	1.3	2.1	2.8	3.6
28	0.8	1.7	2.8	3.4	4.1
32	1.0	2.2	3.6	4.4	4.9
36	1.3	2.9	4.4	4.6	6.8

REFERENCES

1. S. K. Mitchell, N. R. Bedford, and G. E. Ellis, "Multipath Analysis of Explosive Source Signals in the Ocean", J. Acoust. Soc. Am. 67(5), 1582-1589 (1980).

2. J. L. Worzel et al., "Initial Reports of the Deep Sea Drilling Project", Vol. X (U. S. Government Printing Office, Washington, D.C., 1973).

3. E. C. Snow and J. E. Matthews, A Summary of Selected Data: DSDP Legs 1-19, NORDA Rpt. 25, Naval Ocean Research and Development Activity, NSTL Station, Mississippi (1980).

4. E. L. Hamilton, "Sound Velocity-Density Relations in Sea-Floor Sediments and Rocks", J. Acoust. Soc. Am. 63, 366-377 (1978).

5. A. J. Bertagne, "Seismic Stratigraphic Investigation - Western Gulf of Mexico," Masters Thesis, The University of Texas at Austin, Austin, Texas, 1980.

6. A. R. Gregory, "Aspects of Rock Physics from Laboratory and Log Data That Are Important to Seismic Interpretation", in Seismic Stratigraphy - Applications to Hydrocarbon Exploration, edited by C. E. Payton, AAPG Mem. 26, pp. 25-46.

7. J. E. Matthews, "Heuristic Physical Property Model for Marine Sediments," J. Acoust. Soc. Am. 68, 1361-1370 (1980).

8. M. W. Hooper and S. K. Mitchell, "Initial Results of a Study To Determine Bottom Reflection Angles from a Comparison of Signal Arrival Times", Applied Research Laboratories Technical Letter No. 80-19 (ARL-TL-EV-80-19), Applied Research Laboratories, The University of Texas at Austin, 1980.

9. E. L. Hamilton, "Geoacoustic Models of the Sea Floor" in Physics of Sound in Marine Sediments, edited by L. D. Hampton (Plenum Press, New York, 1974).

10. S. K. Mitchell and J. J. Lemmon, "A Ray Theory Model of Acoustic Interaction with the Ocean Bottom", J. Acoust. Soc. Am. 66(3), 855-861 (1979).

11. S. K. Mitchell and K. C. Focke, "New Measurements of Compressional Wave Attenuation in Deep Ocean Sediments", J. Acoust. Soc. Am. 67(5), 1582-1589 (1980).

5 October 1981

DISTRIBUTION LIST FOR
ARL-TR-81-37
UNDER CONTRACT N00014-78-C-0329

Copy No.

Commanding Officer
Naval Ocean Research and Development Activity
NSTL Station, MS 39529

1 Attn: Code 110
2 Code 125L
3 Code 115
4 Code 300
5 Code 320
6 Code 340
7 Code 500
8 Code 520 File
9 Code 530

Commanding Officer
Naval Research Laboratory
Washington, D.C. 20375

10 Attn: Code 8100
11 Code 8160
12 Code 2627

Commander
Naval Oceanographic Office
NSTL Station, Bay St. Louis, MS 39522

13 Attn: Code 7300
14 Code 9210

Commanding Officer
Naval Research Laboratory
Underwater Sound Reference Division
P. O. Box 8337
Orlando, FL 32806

15 Attn: Code 0277
16 Code 8280
17 Code 8289

Naval Ocean Research and Development Activity
Liaison Office
Department of the Navy
Arlington, VA 22217

18 Attn: Code 130

Distribution List for ARL-TR-81-37 under Contract N00014-78-C-0329 (Cont'd)

Copy No.

Officer in Charge
New London Labortory
Naval Underwater Systems Center
New London, CT 06320
19 Attn: L. King
20 P. Herstein

Commander
Naval Ocean Systems Center
San Diego, CA 92152
21 Attn: M. Akers
22 H. Bucher
23 E. Hamilton
24 E. Tunstall

25 Commanding Officer
Naval Coastal Systems Center
Panama City, FL 32407

26 Officer in Charge
Naval Surface Weapons Center
White Oak Laboratory
Silver Spring, MD 20910

27 Officer In Charge
David W. Taylor Naval Ship Research and
Development Center
Carderock Laboratory
Bethesda, MD 20084

28 Director
Naval Ocean Surveillance Information Center
4301 Suitland Road
Washington, D.C. 20390

29 Commanding Officer
Naval Intelligence Support Center
4301 Suitland Road
Washington, D.C. 20390

Superintendent
Naval Postgraduate School
Monterey, CA 93940
30 Attn: Library

Distribution List for ARL-TR-81-37 under Contract N0014-78-C-0329 (Cont'd)

Copy No.

	Assistant Secretary of the Navy Research, Engineering, and Systems Department of the Navy Washington, D.C. 20350
31	Attn: G. A. Cann
	Chief of Naval Operations Department of the Navy Washington, D.C. 20350
32	Attn: OP-02
33	OP-03
34	OP-05
35	OP-095
36	OP-096
37	OP-951
38	OP-952
39	OP-951F
40	OP-952D
	Headquarters Naval Material Command Washington, D.C. 20360
41 -42	Attn: MAT 08T245
	Project Manager Antisubmarine Warfare System Project Department of the Navy Washington, D.C. 20360
43 - 44	Attn: PM-4
	Director Strategic System Project Office Department of the Navy Washington, D.C. 20376
45	Attn: PM-1
	Chief of Naval Research Department of the Navy Arlington, VA 22217
46	Attn: Code 100
47	Code 102B
48	Code 220
49	Code 230
50	Code 460
51	Code 480

Distribution List for ARL-TR-81-37 under Contract N0014-78-C-0329 (Cont'd)

Copy No.

Commanding Officer
Office of Naval Research
ONRDET
NSTL Station
Bay St. Louis, MS 39529
52 Attn: A. Anderson (Code 420D)
53 LCDR M. McDonald (Code 425GG)

Commanding Officer
Office of Naval Research
Branch Office London
FPO New York, NY 09510
54 Attn: Code 241

Commander
Naval Electronic Systems Command
Washington, D. C. 20360
55 Attn: PME 124
56 PME 124TA
57 PME 124/30
58 PME 124/40
59 PME 124/60
60 Code 6[illegible]

Commander
Naval Sea Systems Command
Washington, D.C. 20362
61 Attn: Code 63R-1

Commander
Naval Air Systems Command
Washington, D.C. 20361
62 Attn: Code 370
63 PMA 264

64 Deputy Undersecretary of Defense for
Research and Engineering
Department of Defense
Washington, D.C. 20301

Defense Advanced Research Projects Agency
1400 Wilson Boulevard
Arlington, VA 22209
65 Attn: T. Kooij
66 CDR K. Evans

Distribution List for ARL-TR-81-37 under Contract N00014-78-C-0329 (Cont'd)

Copy No.

Commander
Naval Oceanography Command
NSTL Station, MS 39529
67 Attn: J. Allen

68 Directory of Navy Laboratories
Room 1062, Crystal Plaza, Bldg. 5
Department of the Navy
Washington, D.C. 20360

Commander in Chief
U.S. Atlantic Fleet
Norfolk, VA 23511
69 Attn: Code 353

Commander
Operational Test and Evaluation Force
Naval Base
Norfolk, VA 23511
70 Attn: Code 42

Commander
Oceanographic System, Atlantic
Box 100
Norfolk, VA 23511
71 Attn: LT P. A. Kuhn, N34
72 W. G. Schreiber

73 Oceanographic Development Squadron 8
Naval Air Station
Patuxent River, MD 20670

Commanding Officer
Chesapeake Division
Naval Facilities Engineering Command
Washington Navy Yard
Washington, D.C. 20374
74 Attn: Code FPO-1E4

Defense Advanced Research Projects Agency
ARPA Research Center
Unit 1, Bldg. 301A
NAS Moffett Field, CA 94035
75 Attn: E. L. Smith

Distribution List for ARL-TR-81-37 under Contract N00014-78-C-0329 (Cont'd)

Copy No.

76 - 87	Commanding Officer and Director Defense Technical Information Center Cameron Station, Building 5 5010 Duke Street Alexandria, VA 22314
	Director of Naval Matters Center for Naval Analyses Arlington, VA 22209
88	Attn: C. E. Woods
	Applied Physics Laboratory The Johns Hopkins University Johns Hopkins Road Laurel, MD 20810
89	Attn: A. Chwastyk
90	W. L. May
91	G. L. Smith
92	J. Lombardo
	Woods Hole Oceanographic Institution Woods Hole, MA 02543
93	Attn: E. E. Hayes
	B-K Dynamics, Incorporated 15825 Shady Grove Road Rockville, MD 20850
94	Attn: P. G. Bernard
	Bell Telephone Laboratories, Inc. Whippany Road Whippany, NJ 07961
95	Attn: J. Goldman
96	L. F. Fretwell
	Daubin Systems Corporation 104 Crandon Blvd. Key Biscayne, FL 33149
97	Attn: S. C. Daubin
	Ocean Data Systems, Inc. 6000 Executive Boulevard Rockville, MD 20852
98	Attn: G. V. Jacobs

Distribution List for ARL-TR-81 37 under Contract N00014-78-C-0329 (Cont'd)

Copy No.

Planning Systems Incorporated
7900 Westpark Drive
Suite 600
McLean, VA 22101
99 Attn: R. S. Cavanaugh

Science Applications, Inc.
P. O. Box 1303
McLean, VA 22101
100 Attn: J. S. Hanna
101 C. W. Spofford

Tracor, Inc.
Rockville Laboratory
1601 Research Blvd.
Rockville, MD 20850
102 Attn: J. T. Gottwald

TRW Incorporated
7600 Colshire Drive
McLean, VA 22101
103 Attn: R. T. Brown
104 I. B. Gereben

Western Electric Company, Inc.
P. O. Box 20046
Greensboro, NC 27420
105 Attn: R. H. Harris

106 Office of Naval Research
Resident Representative
Room 582, Federal Building
Austin, TX 78701

107 Environmental Sciences Division, ARL:UT

108 Kenneth E. Hawker, ARL:UT

109 Michael W. Hooper, ARL:UT

110 Gregory D. Ingram, ARL:UT

111 Stephen K. Mitchell, ARL:UT

112 Clark S. Penrod, ARL:UT

113 Jack A. Shooter, ARL:UT

Distribution List for ARL-TR-81-37 under Contract N00014-78-C0329 (Cont'd)

Copy No.

114	Reuben H. Wallace, ARL:UT
115	Library, ARL:UT
116 - 125	Reserve, ARL:UT

DEPARTMENT OF THE NAVY
OFFICE OF NAVAL RESEARCH
875 NORTH RANDOLPH STREET
SUITE 1425
ARLINGTON VA 22203-1995

IN REPLY REFER TO:

5510/1
Ser 321OA/011/06
31 Jan 06

MEMORANDUM FOR DISTRIBUTION LIST

Subj: DECLASSIFICATION OF LONG RANGE ACOUSTIC PROPAGATION PROJECT (LRAPP) DOCUMENTS

Ref: (a) SECNAVINST 5510.36

Encl: (1) List of DECLASSIFIED LRAPP Documents

1. In accordance with reference (a), a declassification review has been conducted on a number of classified LRAPP documents.

2. The LRAPP documents listed in enclosure (1) have been downgraded to UNCLASSIFIED and have been approved for public release. These documents should be remarked as follows:

   Classification changed to UNCLASSIFIED by authority of the Chief of Naval Operations (N772) letter N772A/6U875630, 20 January 2006.

   DISTRIBUTION STATEMENT A: Approved for Public Release; Distribution is unlimited.

3. Questions may be directed to the undersigned on (703) 696-4619, DSN 426-4619.

BRIAN LINK
By direction

Subj: DECLASSIFICATION OF LONG RANGE ACOUSTIC PROPAGATION PROJECT (LRAPP) DOCUMENTS

DISTRIBUTION LIST:

NAVOCEANO (Code N121LC – Jaime Ratliff)
NRL Washington (Code 5596.3 – Mary Templeman)
PEO LMW Det San Diego (PMS 181)
DTIC-OCQ (Larry Downing)
ARL, U of Texas
Blue Sea Corporation (Dr.Roy Gaul)
ONR 32B (CAPT Paul Stewart)
ONR 321OA (Dr. Ellen Livingston)
APL, U of Washington
APL, Johns Hopkins University
ARL, Penn State University
MPL of Scripps Institution of Oceanography
WHOI
NAVSEA
NAVAIR
NUWC
SAIC

Declassified LRAPP Documents

Report Number	Personal Author	Title	Publication Source (Originator)	Pub. Date	Current Availability	Class.
NORDA35VOL.1BK 2OF3	Lauer, R.B.	THE ACOUSTIC MODEL EVALUATION COMMITTEE (AMEC) REPORTS, VOL. 2- APPENDICES A-D- EVALUATION OF THE FACT PL9D TRANSMISSION LOSS MODEL	Naval Ocean R&D Activity	810901	ND ADC034017	U
NORDA36VOL.3BK 2OF3	Lauer, R.B., et al.	THE ACOUSTIC MODEL EVALUATION COMMITTEE (AMEC) REPORTS, VOL. 3- APPENDICES A-D- EVALUATION OF THE RAYMODE X PROPAGATION LOSS MODEL (U)	Naval Ocean R&D Activity	810901	ND ADC034022	U
Unavailable	Hooper, M. W., et al.	MEASUREMENTS AND ANALYSIS OF ACOUSTIC BOTTOM INTERACTION IN THE NORTHWESTERN MEXICAN BASIN	University of Texas, Applied Research Laboratories	811005	ADA107551	U
Unavailable	Kirby, W. D.	FINAL REPORT FOR CONTRACT NUMBER N00014-78-C-0862	Science Applications Inc.	820201	ADA111000	U
Unavailable	Brunson, B. A., et al.	PHYSICAL SEDIMENT MODEL FOR THE PREDICTION OF SEAFLOOR GEOACOUSTIC PROPERTIES	Planning Systems Inc.	820701	ADA119445	U
Unavailable	Cavanagh, R. C., et al.	NORDA PARABOLIC EQUATION WORKSHOP, 31 MARCH - 3 APRIL 1981	Naval Ocean R&D Activity	820901	ADA121932	U
NORDA34VOL.1A	Martin, R. L., et al.	THE ACOUSTIC MODEL EVALUATION COMMITTEE (AMEC) REPORTS, VOL. 1A- SUMMARY OF RANGE INDEPENDENT ENVIRONMENT ACOUSTIC PROPAGATION DATA SETS	Naval Ocean R&D Activity	820901	ADC034017; ND	U
Unavailable	Bartberger, C. L., et al.	THE ACOUSTIC MODEL EVALUATION COMMITTEE (AMEC) REPORTS, VOLUME 2. THE EVALUATION OF	Naval Ocean R&D Activity	820901	ADC034019	U
Unavailable	Deavenport, R., et al.	THE ACOUSTIC MODEL EVALUATION COMMITTEE (AMEC) REPORTS, VOLUME 3. EVALUATION OF THE RAYMODE X PROPAGATION LOSS MODEL. BOOK 2. APPENDICES A-D	Naval Ocean R&D Activity	820901	ADC034022	U
Unavailable	Unavailable	1975-1982 SUMMARY REPORT	Analysis and Technology, Inc.	821217	ADA192591	U
Unavailable	DeChico, D.	ACOUSTIC EVALUATION OF SANDERS ASSOCIATES ACODAC SENSORS	Naval Air Development Center	830301	ADB073873	U
NRL-FR-8695; NRL-8695	Palmer, L. B., et al.	TRANSVERSE HORIZONTAL COHERENCE AND LOW-FREQUENCY ARRAY GAIN LIMITS IN THE DEEP OCEAN	Naval Research Laboratory	830809	ND	U
Unavailable	Unavailable	ENGINEERING SUPPORT FOR ACOUSTIC AND ANALYSIS SYSTEM	Systems Integrated	840101	ADB091112	U
Unavailable	Unavailable	SEAS (SURVEILLANCE ENVIRONMENTAL ACOUSTIC SUPPORT PROGRAM) SUPPORT	Systems Integrated	840229	ADB091119	U